Fig S1

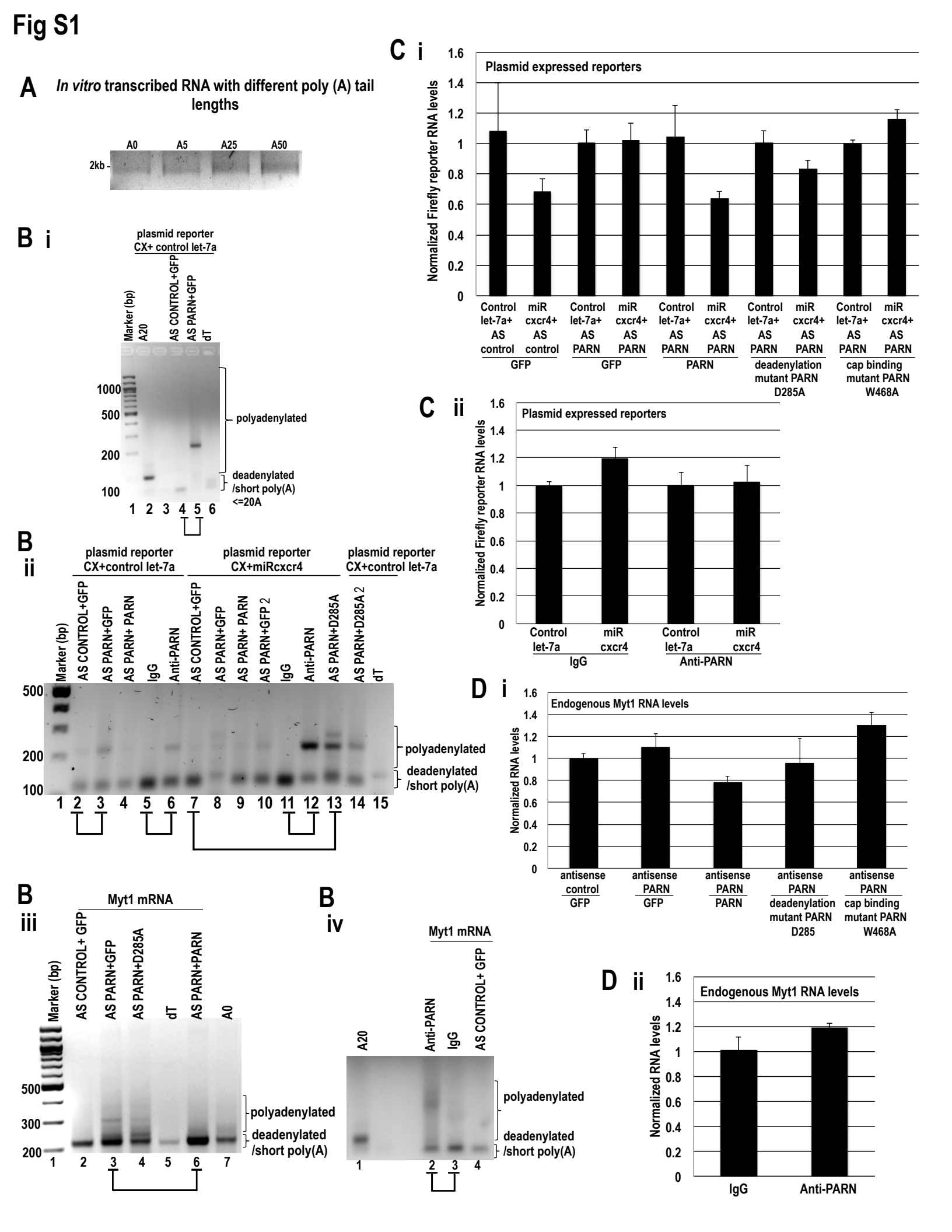
A
In vitro transcribed RNA with different poly (A) tail lengths
A0
A5
A25
A50
2kb
B i
plasmid reporter CX+ control let-7a
Marker (bp)
A20
AS CONTROL+GFP
AS PARN+GFP
dT
1000
500
200
100
polyadenylated
deadenylated /short poly(A) <=20A
1 2 3 4 5 6
B ii
plasmid reporter CX+control let-7a
plasmid reporter CX+miRcxcr4
plasmid reporter CX+control let-7a
Marker (bp)
AS CONTROL+GFP
AS PARN+GFP
AS PARN+ PARN
IgG
Anti-PARN
AS CONTROL+GFP
AS PARN+GFP
AS PARN+ PARN
AS PARN+GFP 2
IgG
Anti-PARN
AS PARN+D285A
AS PARN+D285A 2
dT
500
200
100
polyadenylated
deadenylated /short poly(A)
1 2 3 4 5 6 7 8 9 10 11 12 13 14 15
B iii
Myt1 mRNA
Marker (bp)
AS CONTROL+ GFP
AS PARN+GFP
AS PARN+D285A
dT
AS PARN+PARN
A0
500
300
200
polyadenylated
deadenylated /short poly(A)
1 2 3 4 5 6 7
B iv
Myt1 mRNA
A20
Anti-PARN
IgG
AS CONTROL+ GFP
polyadenylated
deadenylated /short poly(A)
1 2 3 4
C i
Plasmid expressed reporters
Normalized Firefly reporter RNA levels
1.6
1.4
1.2
1
0.8
0.6
0.4
0.2
0
Control let-7a+ AS control
miR cxcr4+ AS control
Control let-7a+ AS PARN
miR cxcr4+ AS PARN
Control let-7a+ AS PARN
miR cxcr4+ AS PARN
Control let-7a+ AS PARN
miR cxcr4+ AS PARN
Control let-7a+ AS PARN
miR cxcr4+ AS PARN
GFP
GFP
PARN
deadenylation mutant PARN D285A
cap binding mutant PARN W468A
C ii
Plasmid expressed reporters
Normalized Firefly reporter RNA levels
1.6
1.4
1.2
1
0.8
0.6
0.4
0.2
0
Control let-7a
miR cxcr4
Control let-7a
miR cxcr4
IgG
Anti-PARN
D i
Endogenous Myt1 RNA levels
Normalized RNA levels
1.6
1.4
1.2
1
0.8
0.6
0.4
0.2
0
antisense control GFP
antisense PARN GFP
antisense PARN PARN
antisense PARN deadenylation mutant PARN D285
antisense PARN cap binding mutant PARN W468A
D ii
Endogenous Myt1 RNA levels
Normalized RNA levels
1.6
1.4
1.2
1
0.8
0.6
0.4
0.2
0
IgG
Anti-PARN

Fig S2

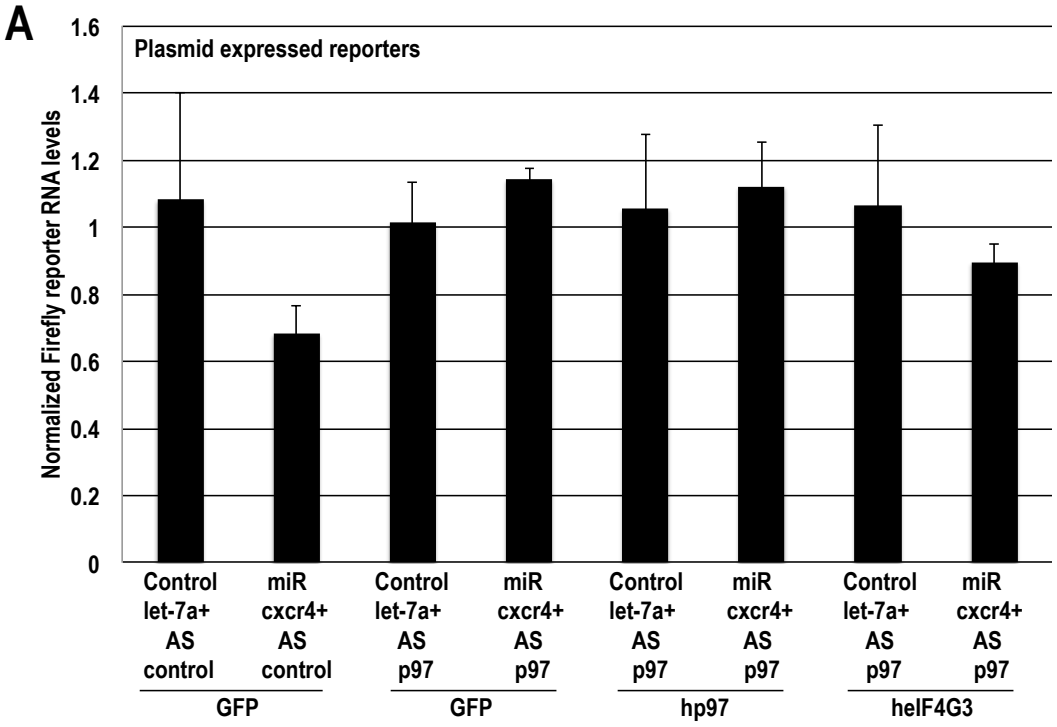
A
Plasmid expressed reporters
Normalized Firefly reporter RNA levels
1.6
1.4
1.2
1
0.8
0.6
0.4
0.2
0
Control let-7a+ AS control
miR cxcr4+ AS control
Control let-7a+ AS p97
miR cxcr4+ AS p97
Control let-7a+ AS p97
miR cxcr4+ AS p97
Control let-7a+ AS p97
miR cxcr4+ AS p97
GFP
GFP
hp97
heIF4G3

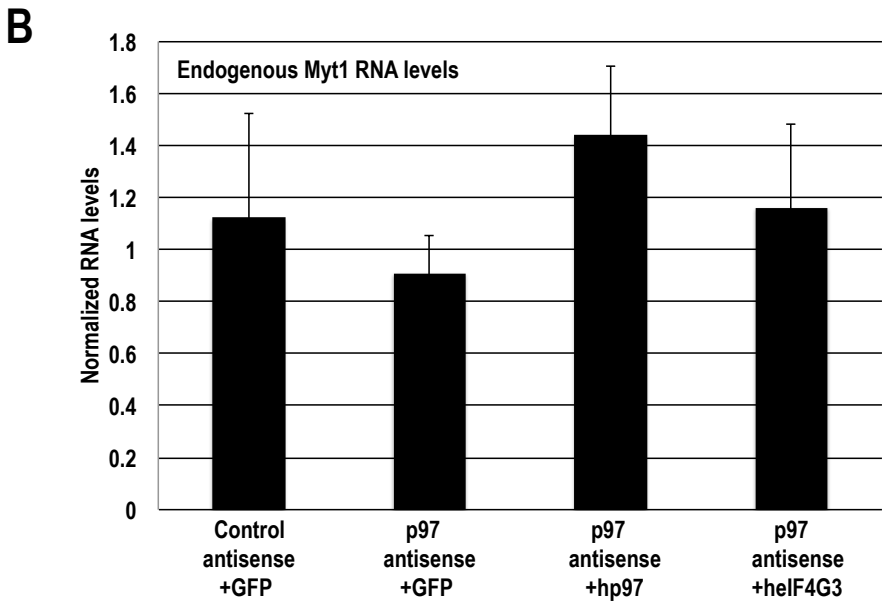
B
Endogenous Myt1 RNA levels
Normalized RNA levels
1.8
1.6
1.4
1.2
1
0.8
0.6
0.4
0.2
0
Control antisense +GFP
p97 antisense +GFP
p97 antisense +hp97
p97 antisense +heIF4G3

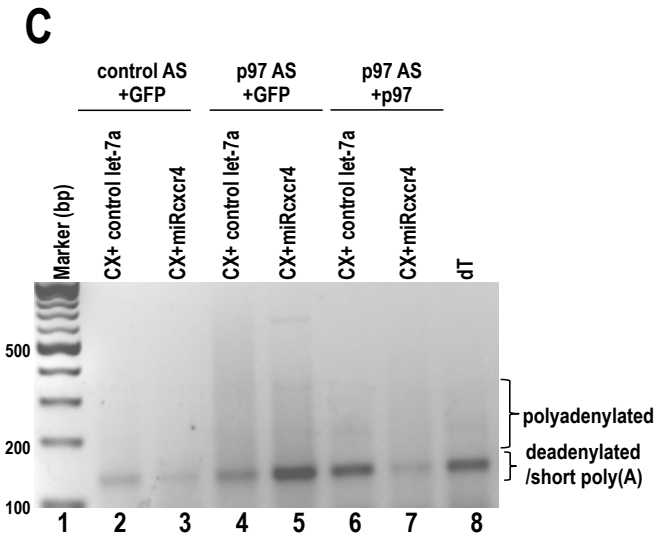
C
control AS +GFP
p97 AS +GFP
p97 AS +p97
Marker (bp)
CX+ control let-7a
CX+miRcxcr4
CX+ control let-7a
CX+miRcxcr4
CX+ control let-7a
CX+miRcxcr4
dT
500
200
100
polyadenylated
deadenylated /short poly(A)
1 2 3 4 5 6 7 8

Fig S3

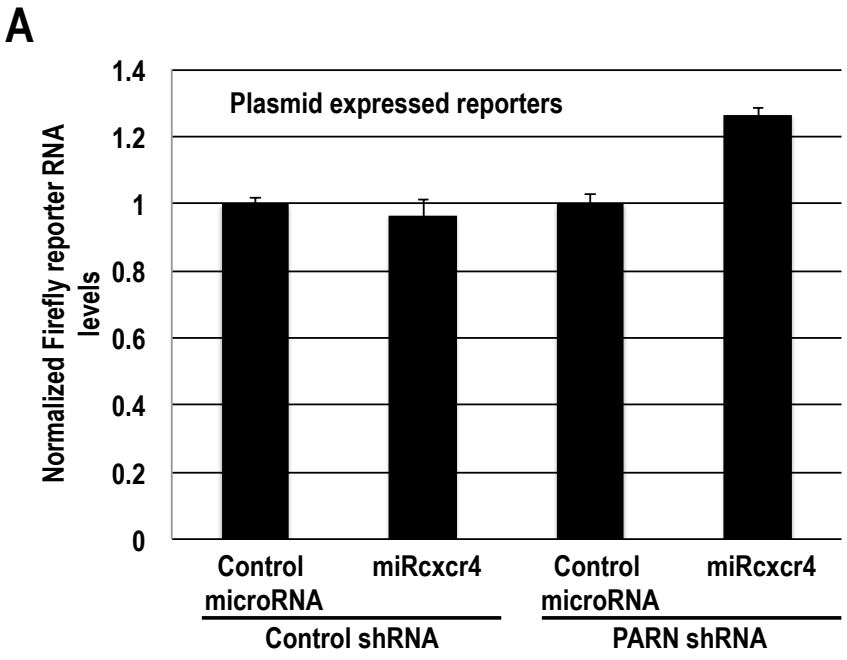
A
Plasmid expressed reporters
Normalized Firefly reporter RNA levels
1.4
1.2
1
0.8
0.6
0.4
0.2
0
Control microRNA
miRcxcr4
Control microRNA
miRcxcr4
Control shRNA
PARN shRNA

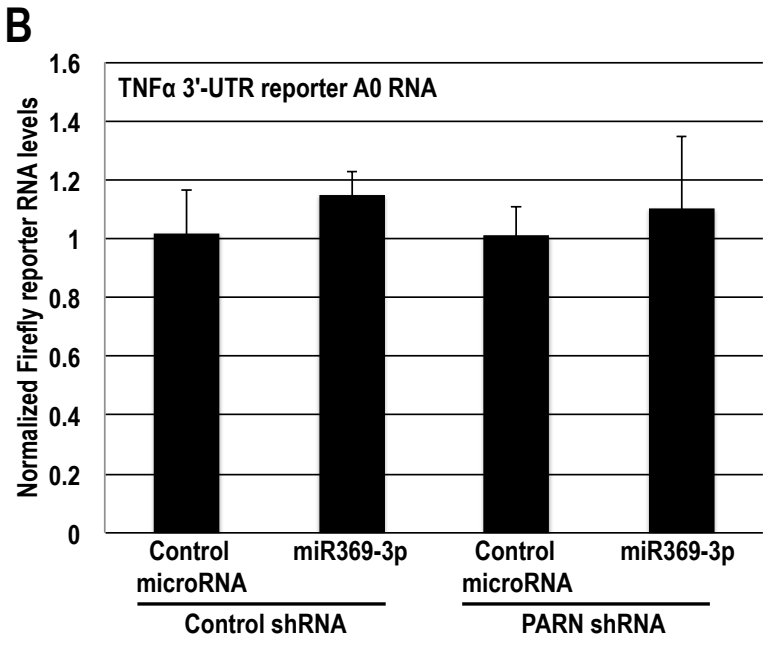
B
TNFα 3'-UTR reporter A0 RNA
Normalized Firefly reporter RNA levels
1.6
1.4
1.2
1
0.8
0.6
0.4
0.2
0
Control microRNA
miR369-3p
Control microRNA
miR369-3p
Control shRNA
PARN shRNA

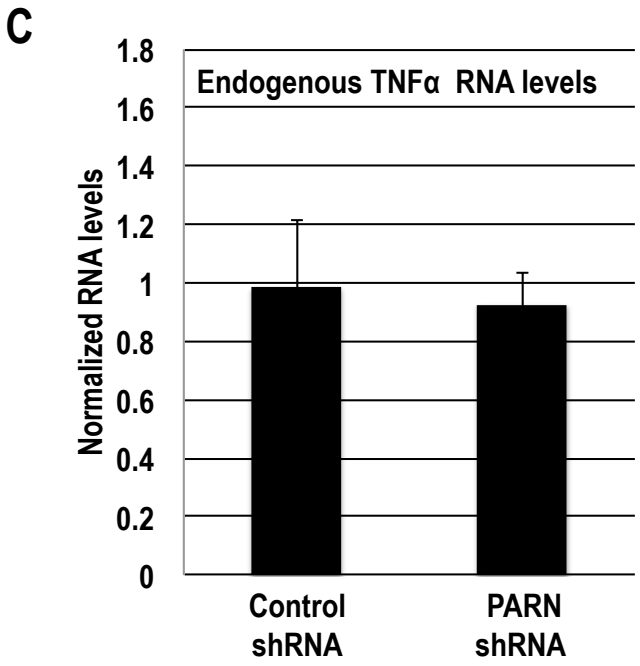
C
Endogenous TNFα RNA levels
Normalized RNA levels
1.8
1.6
1.4
1.2
1
0.8
0.6
0.4
0.2
0
Control shRNA
PARN shRNA

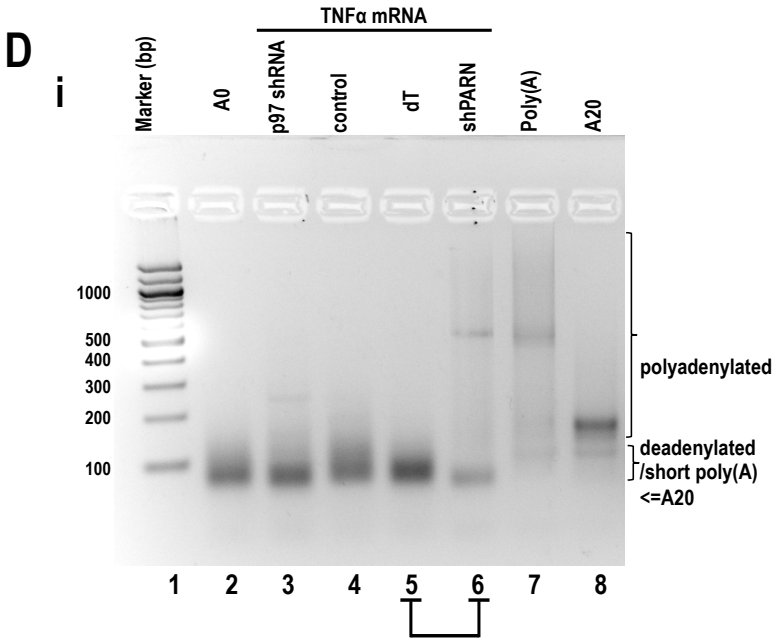
D i
TNFα mRNA
Marker (bp)
A0
p97 shRNA
control
dT
shPARN
Poly(A)
A20
1000
500
400
300
200
100
polyadenylated
deadenylated /short poly(A) <=A20
1 2 3 4 5 6 7 8

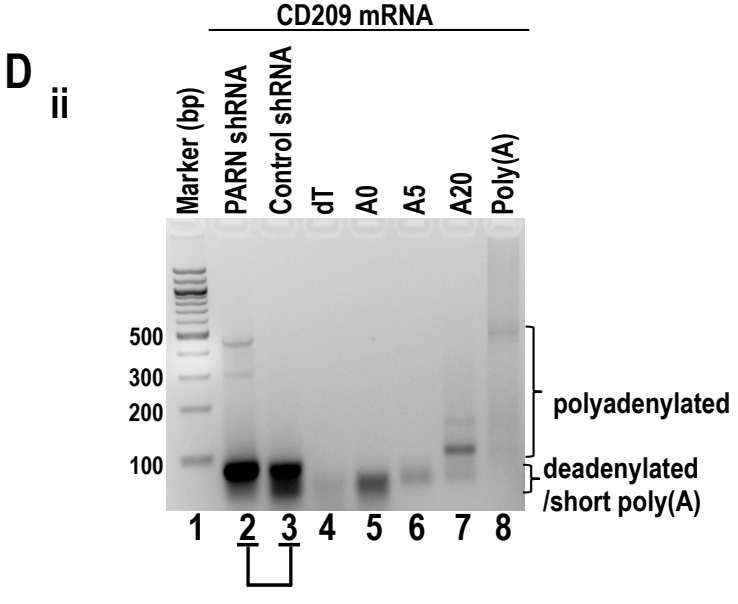
D ii
CD209 mRNA
Marker (bp)
PARN shRNA
Control shRNA
dT
A0
A5
A20
Poly(A)
500
300
200
100
polyadenylated
deadenylated /short poly(A)
1 2 3 4 5 6 7 8

Fig S4

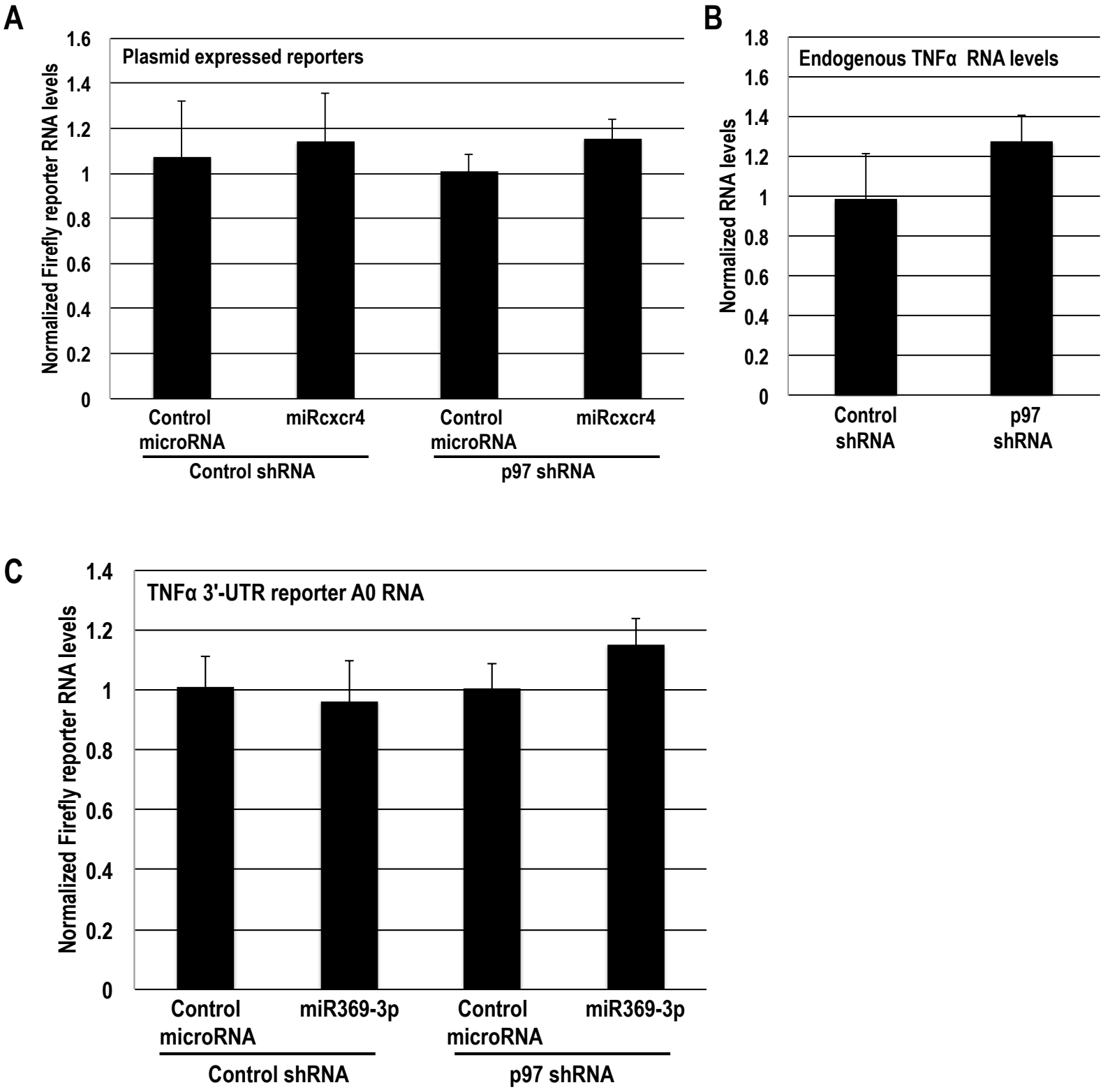
A
Plasmid expressed reporters
Normalized Firefly reporter RNA levels
1.6
1.4
1.2
1
0.8
0.6
0.4
0.2
0
Control microRNA
miRcxcr4
Control microRNA
miRcxcr4
Control shRNA
p97 shRNA
B
Endogenous TNFα RNA levels
Normalized RNA levels
1.8
1.6
1.4
1.2
1
0.8
0.6
0.4
0.2
0
Control shRNA
p97 shRNA
C
TNFα 3'-UTR reporter A0 RNA
Normalized Firefly reporter RNA levels
1.4
1.2
1
0.8
0.6
0.4
0.2
0
Control microRNA
miR369-3p
Control microRNA
miR369-3p
Control shRNA
p97 shRNA

Fig S5

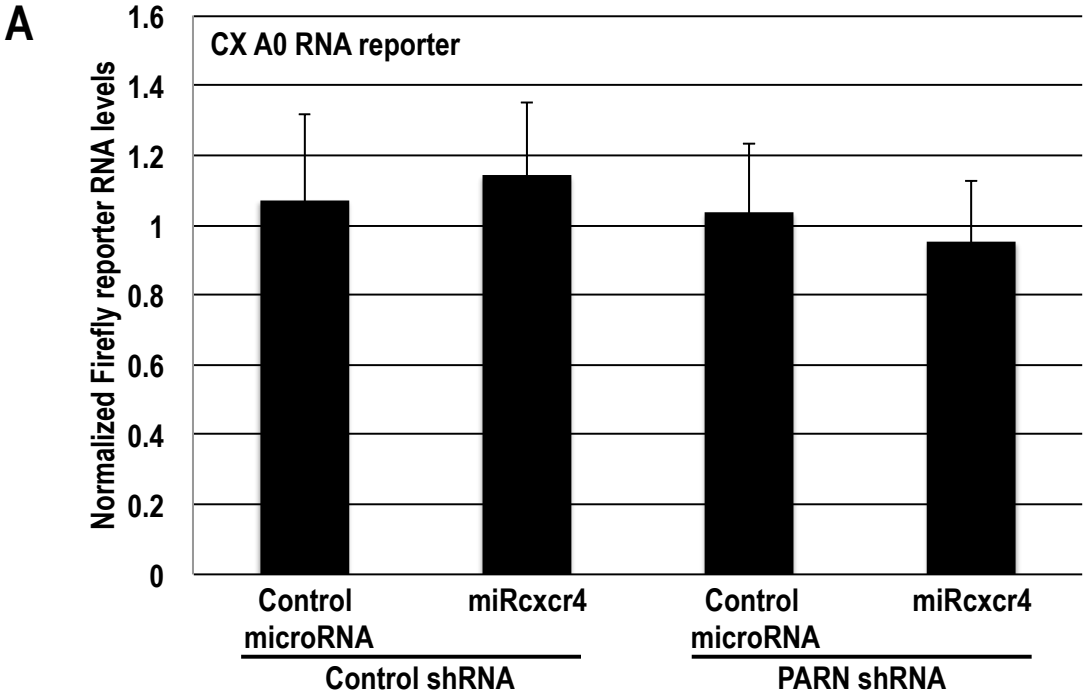
A
CX A0 RNA reporter
Normalized Firefly reporter RNA levels
1.6
1.4
1.2
1
0.8
0.6
0.4
0.2
0
Control microRNA
miRcxcr4
Control microRNA
miRcxcr4
Control shRNA
PARN shRNA

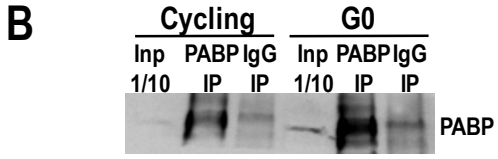
B
Cycling
G0
Inp 1/10
PABP IP
IgG IP
Inp 1/10
PABP IP
IgG IP
PABP

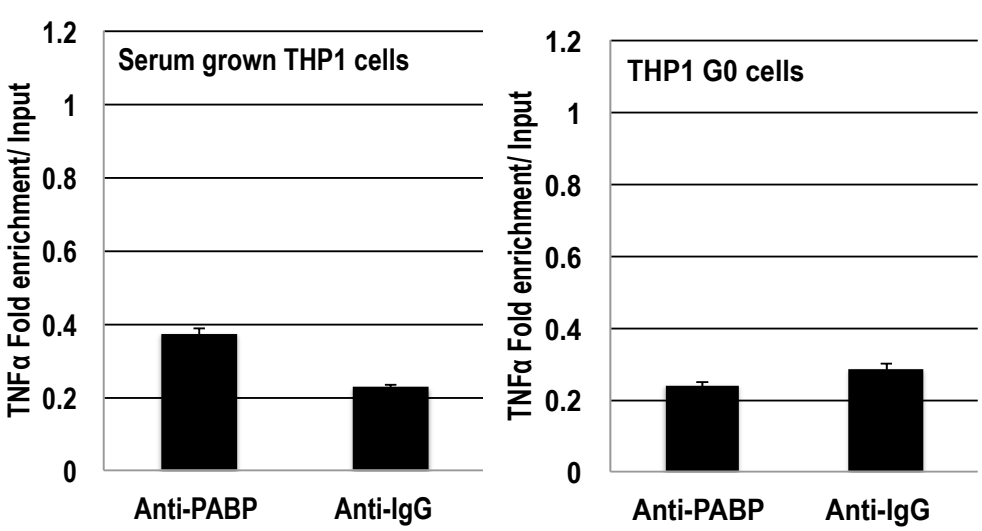
C
Serum grown THP1 cells
TNFα Fold enrichment/ Input
1.2
1
0.8
0.6
0.4
0.2
0
Anti-PABP
Anti-IgG
THP1 G0 cells
TNFα Fold enrichment/ Input
1.2
1
0.8
0.6
0.4
0.2
0
Anti-PABP
Anti-IgG

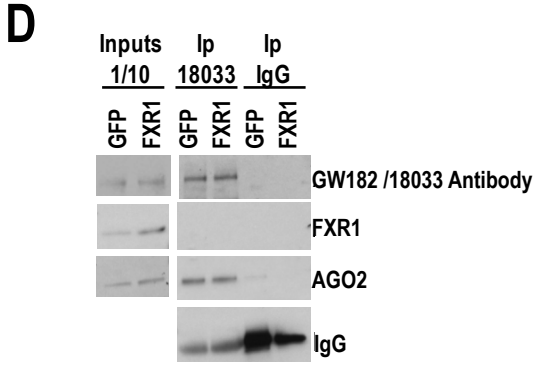
D
Inputs 1/10
Ip 18033
Ip IgG
GFP
FXR1
GFP
FXR1
GFP
FXR1
GW182 /18033 Antibody
FXR1
AGO2
IgG

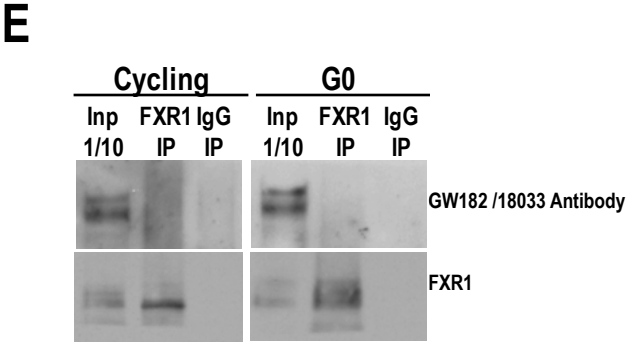
E
Cycling
G0
Inp 1/10
FXR1 IP
IgG IP
Inp 1/10
FXR1 IP
IgG IP
GW182 /18033 Antibody
FXR1

Fig S6

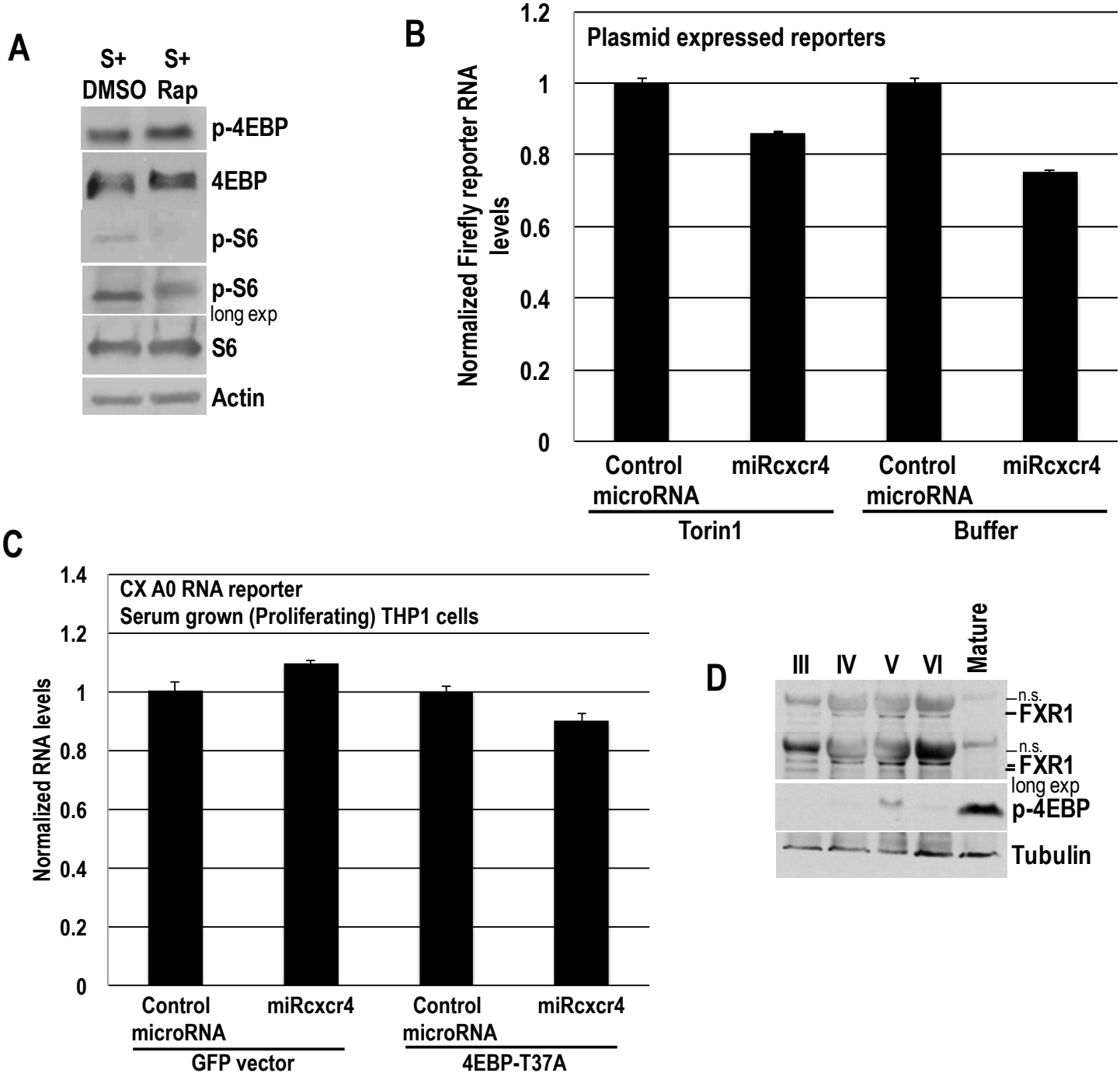
A
S+ DMSO
S+ Rap
p-4EBP
4EBP
p-S6
p-S6 long exp
S6
Actin
B
Plasmid expressed reporters
Normalized Firefly reporter RNA levels
1.2
1
0.8
0.6
0.4
0.2
0
Control microRNA
miRcxcr4
Control microRNA
miRcxcr4
Torin1
Buffer
C
CX A0 RNA reporter
Serum grown (Proliferating) THP1 cells
Normalized RNA levels
1.4
1.2
1
0.8
0.6
0.4
0.2
0
Control microRNA
miRcxcr4
Control microRNA
miRcxcr4
GFP vector
4EBP-T37A
D
III
IV
V
VI
Mature
n.s.
FXR1
n.s.
FXR1
long exp
p-4EBP
Tubulin

Fig S7

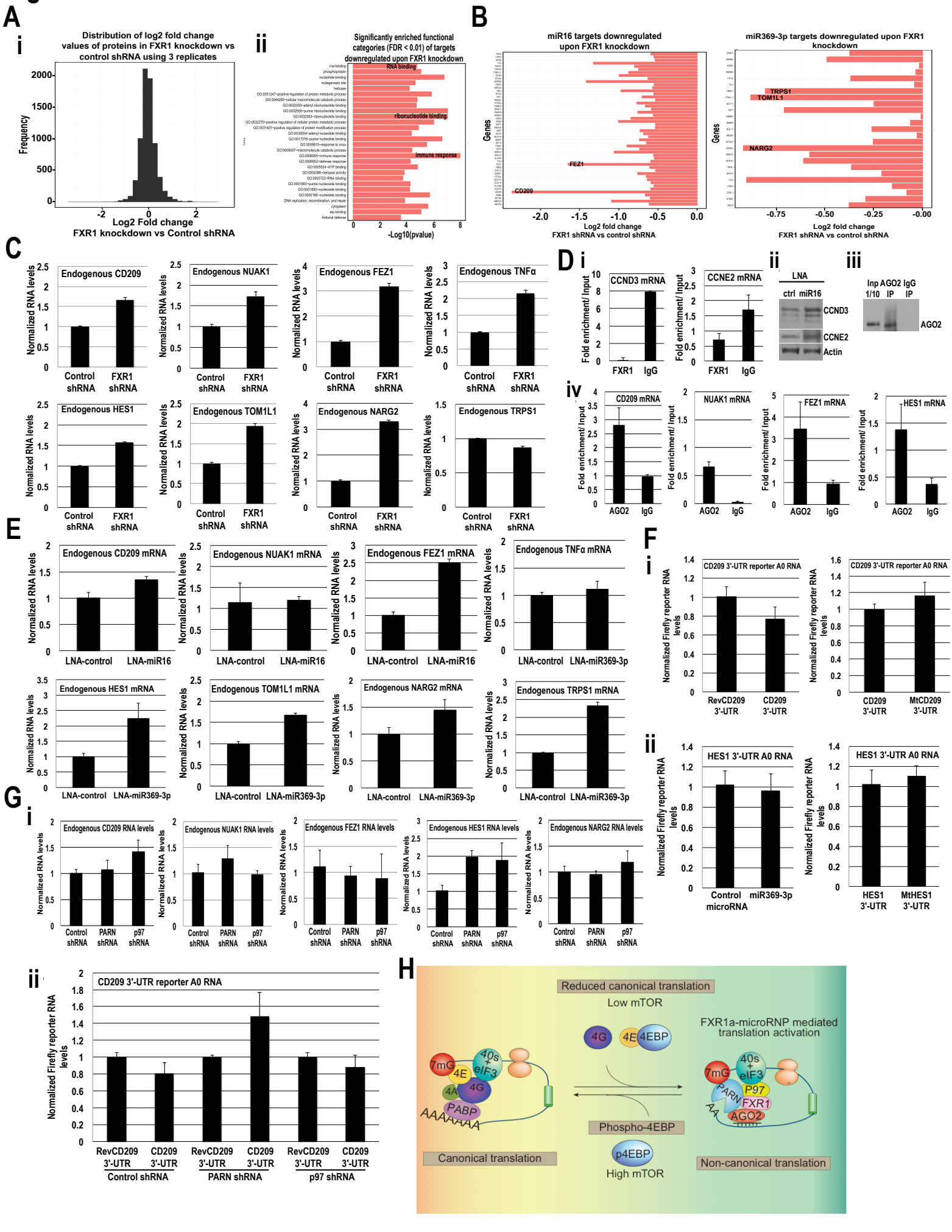
A
i
Distribution of log2 fold change values of proteins in FXR1 knockdown vs control shRNA using 3 replicates
Frequency
Log2 Fold change FXR1 knockdown vs Control shRNA
ii
Significantly enriched functional categories (FDR < 0.01) of targets downregulated upon FXR1 knockdown
RNA binding
ribonucleotide binding
immune response
-Log10(pvalue)
B
miR16 targets downregulated upon FXR1 knockdown
FEZ1
CD209
Genes
Log2 fold change FXR1 shRNA vs control shRNA
miR369-3p targets downregulated upon FXR1 knockdown
TRPS1
TOM1L1
NARG2
C
Endogenous CD209
Endogenous NUAK1
Endogenous FEZ1
Endogenous TNFα
Endogenous HES1
Endogenous TOM1L1
Endogenous NARG2
Endogenous TRPS1
Normalized RNA levels
Control shRNA
FXR1 shRNA
D
i
CCND3 mRNA
CCNE2 mRNA
Fold enrichment/ Input
FXR1
IgG
ii
LNA
ctrl miR16
CCND3
CCNE2
Actin
iii
Inp AGO2 IgG
1/10 IP IP
AGO2
iv
CD209 mRNA
NUAK1 mRNA
FEZ1 mRNA
HES1 mRNA
AGO2
IgG
E
Endogenous CD209 mRNA
Endogenous NUAK1 mRNA
Endogenous FEZ1 mRNA
Endogenous TNFα mRNA
Endogenous HES1 mRNA
Endogenous TOM1L1 mRNA
Endogenous NARG2 mRNA
Endogenous TRPS1 mRNA
Normalized RNA levels
LNA-control
LNA-miR16
LNA-miR369-3p
F
i
CD209 3'-UTR reporter A0 RNA
Normalized Firefly reporter RNA levels
RevCD209 3'-UTR
CD209 3'-UTR
MtCD209 3'-UTR
ii
HES1 3'-UTR A0 RNA
Control microRNA
miR369-3p
HES1 3'-UTR
MtHES1 3'-UTR
G
i
Endogenous CD209 RNA levels
Endogenous NUAK1 RNA levels
Endogenous FEZ1 RNA levels
Endogenous HES1 RNA levels
Endogenous NARG2 RNA levels
Normalized RNA levels
Control shRNA
PARN shRNA
p97 shRNA
ii
CD209 3'-UTR reporter A0 RNA
Normalized Firefly reporter RNA levels
RevCD209 3'-UTR
CD209 3'-UTR
Control shRNA
PARN shRNA
p97 shRNA
H
Reduced canonical translation
Low mTOR
4G
4E
4EBP
7mG
40s
eIF3
4A
PABP
AAAAAAA
FXR1a-microRNP mediated translation activation
PARN
P97
FXR1
AGO2
AA
Phospho-4EBP
p4EBP
High mTOR
Canonical translation
Non-canonical translation

SI Figure Legends

Figure S1. Related to Figure 1. Depletion of PARN in oocytes affects the poly(A) tail lengths of target mRNAs A. ARCA capped CX mRNA transcribed with no poly(A) tail (A0), A5, A25, A50 (CXpA) (Mortensen et al., 2011). **B. i.** PAT assay (SI extended procedures; (Bazzini et al., 2012; Chang et al., 2014)) of CX mRNA expressed from CMV promoter expressed plasmids injected into immature oocytes treated with control antisense (AS control)+GFP or PARN antisense (AS PARN)+GFP. CX mRNA show extended poly(A) tails upon PARN depletion and short poly (A) tails (<20As) in oocytes without PARN depletion (lanes 5 versus 4) compared to control A20 mRNA (lane 2) and to an RNA sample (antisense PARN+GFP) treated with oligo dT and RNAse H (marked as dT, lane 6) to reduce the poly(A) tail. **ii.** PAT assay of CX mRNA in the samples from Fig. 1E , treated with control antisense+GFP, PARN antisense+GFP, PARN antisense+PARN, PARN antisense+GFP (2, second sample), oocytes treated with IgG control antibody, oocytes treated with anti-PARN antibody, and PARN antisense+PARN D285A. Extended poly(A) tails are observed on CX mRNA upon PARN inhibition with anti-PARN antibody (lanes 12 versus 11, 6 versus 5), upon PARN depletion (lanes 3 versus 2), and with the deadenylase inactive PARN D285A (in place of endogenous PARN in PARN depleted oocytes, lanes 13 versus 7)—compared to short poly(A) tails in oocytes with IgG injection (lanes 11, 5), without PARN depletion (lanes 7, 2), with PARN restored (lane 9) or an RNA sample treated with oligo dT and RNAse H (marked as dT, lane 15) to remove the poly(A) tail as a control. The assay is a non-quantitative PCR based assay. Separate qRT-PCR (C described below) of the same RNA samples shows that RNA levels do not change correspondingly with poly(A) tail length changes and the differences in poly(A) tail forms is not due to changes in total RNA levels. **iii.** PAT assay of endogenous Myt1 mRNA in oocytes from Fig. 1D, treated with control antisense+GFP, PARN antisense+GFP, PARN antisense+PARN or PARN antisense+PARN D285A. Extended poly(A) tails are observed on

Myt1 mRNA upon PARN depletion and with the deadenylase inactive PARN D285A compared to PARN restoration (lanes 3, 4 versus 6), or compared to short poly(A) tails in oocytes without PARN depletion (lane 2), or to control A0 mRNA (lane 7), or an RNA sample treated with oligo dT and RNAse H (dT) to remove the poly(A) tail as a control (lane 5). **iv.** PAT assay of endogenous Myt1 mRNA in oocyte samples from Fig. 1E shows extended poly(A) tails when treated with anti-PARN antibody compared with IgG control (lanes 2 versus 3) or compared with control antisense+GFP (lane 4) or an A20 control (lane 1). Separate qRT-PCR (D described below) of the same RNA samples shows that RNA levels do not change correspondingly with poly(A) tail length changes and the differences in poly(A) tail forms is not due to changes in total RNA levels. **C.** RNA levels by qRT-PCR analysis, of CX Firefly reporter mRNA, normalized to Renilla mRNA, in oocytes injected with control let-7a or miRcxcr4 and **i.** with and without PARN depletion, or complementation with wildtype PARN, D285A or W468A mutants and **ii.** with and without anti-PARN antibody inhibition. RNA levels do not correspond to the changes in Luciferase translation observed upon PARN depletion/mutation in Fig. 1E and to the altered poly(A) tail forms observed upon PARN depletion/mutation in Fig. S1Bi-ii. The effect of PARN depletion/mutation on CX reporter expression is not due to mRNA level changes. **D.** RNA levels by qRT-PCR analysis, of the endogenous target of miR16 for translation activation, Myt1 mRNA—normalized to endogenous xl-tRNA-lys, in oocytes **i.** with and without PARN depletion, or complementation with wildtype PARN, D285A or W468A mutants and **ii.** with and without anti-PARN inhibition. RNA levels do not correspond to the changes in MYT1 protein level observed upon PARN depletion/mutation in Fig. 1D or to the altered poly(A) tail forms observed upon PARN depletion/mutation in Fig. S1Biii-iv. The effect of PARN depletion/mutation on MYT1 expression is not due to mRNA level changes.

Figure S2. Related to Figure 2. RNA levels of reporters and endogenous target mRNA do not correspond with the changes in Luciferase activity/translation and target protein levels upon p97 depletion in oocytes A. RNA levels by qRT-PCR analysis, of CX Firefly reporter mRNA, normalized to Renilla mRNA, in oocytes from Fig. 2A, injected with control let-7a or miRcxcr4, and with/without p97 depletion, and complementation with GFP, human p97 or eIF4G3. **B.** RNA levels by qRT-PCR analysis, of an endogenous target of miR16 for translation activation, Myt1 mRNA, normalized to endogenous xl-tRNA-lys, in oocytes with and without p97 depletion, and complementation with GFP, human p97 or eIF4G3. RNA levels do not change significantly, indicating that the effect of p97 depletion on MYT1 protein level changes is not due to mRNA levels. **C.** PAT assay of CX mRNA in the samples from Fig. 2A, treated with control antisense+GFP, p97 antisense+GFP, and p97 antisense+human p97. Mild to insignificant differences upon p97 depletion is observed by faint extended smearing bands (lane 4 versus lane 6), compared to an RNA sample treated with oligo dT and RNAse H (lane 8) to remove the poly(A) tail as a control.

Figure S3. Related to Figure 3. PARN knockdown affects the poly(A) tail lengths of endogenous activation target mRNAs, TNFα, without affecting RNA levels qRT-PCR analysis of Luciferase mRNA levels normalized to Renilla mRNA levels in control and PARN knockdown G0 cells with miRcxcr4 and control microRNA, miR30a, of **A.** CX reporter mRNA from Figure 3D. **B.** of TNFα 3′-UTR reporter Luciferase A0 mRNA from Figure 3E. **C.** qRT-PCR analysis of endogenous TNFα mRNA levels normalized to endogenous tRNA-lys in control and PARN knockdown G0 cells. These RNA levels in control and PARN knockdown cells do not change significantly and do not account for the decrease in Luciferase activity (Fig. 3D-E) and endogenous TNFα levels (Fig.7Fi). **D.** PAT assay of endogenous targets: **i.** TNFα mRNA, from G0 cells with and without p97 or PARN knockdown. Extended poly(A)

tails are observed upon PARN depletion (lane 6), similar to a control poly(A) mRNA (lane 7), while short poly(A) tails (<20As) are observed in control shRNA cells without PARN depletion (lane 4), compared to an RNA sample treated with oligo dT and RNAse H to remove the poly(A) tail as a control (lane 5), and compared to control A0, A20 mRNAs (lanes 2, 8); mild, insignificant differences are observed with or without p97 knockdown (lanes 3 verus 4). **ii.** PAT assay of CD209 mRNA, from G0 cells with and without PARN knockdown (lanes 2 versus 3). Extended poly(A) tail forms are observed upon PARN depletion (lane 2) and with control poly(A) mRNA (lane 8), compared to short poly(A) tails (<20As) in control shRNA cells (lane 3), and compared to control A0, A5, A20 mRNAs (lanes 5-7), and an RNA sample treated with oligo dT and RNAse H to remove the poly(A) tail as a control (lane 4). The assay is a non-quantitative PCR based assay. Separate qRT-PCR (C above and Fig. S4B for TNFα mRNA upon p97 depletion and Fig. S7Gi for CD209) of the same RNA samples shows that the differences in poly(A) tail forms is not due to changes in RNA levels.

Figure S4. Related to Figure 4. RNA levels of reporters and endogenous target mRNA do not change upon p97 knockdown A. qRT-PCR analysis of CX Luciferase reporter mRNA levels in control and p97 knockdown G0 cells with miRcxcr4 and control microRNA, miR30a, from Fig. 4D. Firefly-CX target mRNA levels were normalized to control Renilla mRNA levels. **B.** qRT-PCR analysis of endogenous TNFα mRNA levels normalized to endogenous tRNA-lys in control and p97 knockdown G0 cells. **C.** qRT-PCR analysis of TNFα 3′-UTR reporter Luciferase A0 mRNA levels normalized to control Renilla mRNA levels in control and p97 knockdown G0 cells, from Fig. 4E. These RNA levels in control and p97 knockdown cells do not change significantly and do not account for the decrease in Luciferase activity (Fig. 4D-E) and endogenous TNFα levels (Fig.7Fi).

Figure S5. Related to Figure 5. PABP, which is not part of the activation complex, does not immunoprecipitate TNFα mRNA in G0. GW182, a key factor for microRNA-mediated repression and downregulation, and FXR1, the essential factor for microRNA-mediated activation, do not interact A. qRT-PCR analysis of Luciferase CX A0 mRNA levels normalized to Renilla mRNA levels in control and PARN knockdown G0 cells with miRcxcr4 and control microRNA, miR30a, from Fig. 5A. RNA levels in these control and PARN knockdown cells do not reflect the translation in Fig. 5A. **B.** Western analysis of PABP immunoprecipitation from serum-grown and G0 THP1 cells with IgG as control immunoprecipitation antibody and 10% Input. **C.** PABP and IgG immunoprecipitates were probed for endogenous TNFα mRNA by qRT-PCR relative to Input levels. TNFα mRNA associates with PABP in serum-grown cells (1.8 fold over IgG background) but not significantly in G0 cells (less than/equal to IgG background), where TNFα is expressed by microRNA-mediated activation, has a shortened poly(A) tail (Fig. 3B), and PABP is not associated with factors involved in activation, p97 and PARN (Fig. 4B, 5E), and is not part of the activation complex. **D.** Immunoprecipitation of GW182 (IP 18033; (Yang et al., 2004)) from cytoplasmic lysates of cells expressing GFP or FXR1 followed by Western analysis of GW182 (GW182/18033 antibody), FXR1 and AGO2 reveals no interaction of GW182 with FXR1; AGO2 immunoprecipitates with GW182 antibody as expected. **E.** Immunoprecipitation of FXR1 from total extracts (nuclear and cytoplasmic lysates combined to observe both nuclear and cytoplasmic proteins that may be missing in cytoplasmic lysates (Truesdell et al., 2012)) of in vivo crosslinked proliferating and G0 cells, followed by Western analysis of FXR1 and GW182, reveals no interaction of GW182 (GW182/18033 antibody) with FXR1. IgG=control for immunoprecipitation. 18033 antibody reports not only GW182 levels but can also detect the co-migrating P body protein, Ge-1 (Yu et al., 2005). Multiple bands are observed with GW182 and FXR1 that may be due to modifications or splice isoforms. These bands are observed in total lysates (nuclear+cytoplasmic)

from in vivo crosslinked cells but not from non-crosslinked cytoplasmic lysates in D. In both cases, GW182 does not interact with FXR1.

Figure S6. Related to Figure 6. Target reporter RNA levels do not change with mTOR and 4EBP alteration. FXR1 and phospho-4EBP levels are altered in oocyte stages, similar to THP1 G0 cells A. Western analysis of THP1 cells treated with DMSO or Rapamycin for 2 days and probed for 4EBP and S6 phosphorylation (p-4EBP and p-S6). Total 4EBP, S6, and Actin=loading controls. 4EBP is not significantly dephosphorylated (when normalized to either total 4EBP or Actin) while S6 phosphorylation decreases (4 fold and 5 fold when normalized to total S6 and Actin) with rapamycin as also previously shown (Thoreen et al., 2009; Thoreen et al., 2012; Gingras et al., 1999; Fonseca et al., 2014; Hsieh et al., 2012; Choo et al., 2008; Muranen et al., 2012; Feldman et al., 2009). **B.** qRT-PCR analysis of Luciferase mRNA levels in Torin 1 and NMP buffer treated serum grown cells with control miR30a and miRcxcr4 from Fig. 6B. Firefly-CX target mRNA levels were normalized to control Renilla mRNA levels. No significant differences in RNA levels were observed between buffer and Torin 1 treated cells. **C.** qRT-PCR analysis of CX Luciferase A0 mRNA levels with control miR30a and miRcxcr4, in serum-grown cells, with expression of GFP or eIF4EBP-T37A mutant (from Fig. 6C). Firefly-CX target mRNA levels were normalized to control Renilla mRNA levels. No significant differences in RNA levels were observed between expression of GFP and eIF4EBP-T37A mutant. **D.** FXR1 and phospho-4EBP levels are regulated across oocyte stages. Western analysis of immature oocyte stages III-VI (defolliculated prior to extract preparation), and mature oocytes probed for FXR1 (Abcam), and p-4EBP, with Tubulin as a loading control. n.s.=non-specific signal from yolk proteins. FXR1 runs as multiple bands, which are differentially increased between stages III to VI compared to mature oocytes.

Figure S7. Related to Figure 7. Identification of targets of microRNA-mediated activation. A potential model for the specialized mechanism of microRNA-mediated translation activation by FXR1a-microRNP in low mTOR activity conditions in immature oocytes and in THP1 G0 cells A. i. Histogram showing the distribution of log2 fold change values of proteins in FXR1 knockdown compared to control shRNA G0 (serum-starved for 2 days) THP1 cells based on mass spectrometry analysis of 3 biological replicates (Table S1). **ii.** Significantly enriched functional categories (False discovery rate FDR<0.01) among target genes downregulated upon FXR1 knockdown, based on mass spectrometry analysis (DAVID analysis of protein set with $\geq$ 1.5 fold decrease in FXR1 knockdown compared to control cells, from Table S3). Enlarged version in Table S3. **B.** Top miR16 and miR369-3p targets predicted by the MiRror program (Friedman and Linial, 2013), which are downregulated upon FXR1 knockdown based on mass spectrometry analysis (Tables S4-S5, sheet 6). MiR16 and miR369-3p associate not only with AGO2 but also with FXR1 (Fig. 7Biii), indicating a role in activation, apart from their known role in repression (Liu et al., 2008; Wang et al., 2009; Rissland et al., 2011) through repressive GW182-microRNPs that do not associate with FXR1 in these cells (Fig. S5D-E). **C.** qRT-PCR analysis of total RNA levels of candidate target mRNAs tested in Fig. 7Aiii for polysome association in FXR1 knockdown and control shRNA G0 cells, normalized to tRNA-lys or to Actin mRNA (for NUAK1, NARG2, HES1 and TRPS1 normalization). The total RNA levels of the candidate target mRNAs do not decrease and therefore, do not cause the decrease in polysome association of these mRNAs in FXR1 knockdown cells compared to control shRNA G0 cells shown in Fig. 7Aiii; instead some targets show increase in total RNA levels upon FXR1 knockdown, observed even with normalization to multiple different loading control RNAs. This may be due to indirect stabilization of the mRNAs upon loss of the translation of these mRNAs in FXR1 knockdown cells (their protein levels and polysome association decrease, Table S1, Fig. 7Aiii, indicating loss of translation). **D. i.** FXR1

immunoprecipitation (Fig. 7Bii) does not reveal association of CCND3 and CCNE2 mRNA, which serve as negative controls as they are not targets of activation (Table S1, S4, S7). **ii.** Western analysis of CCND3 and CCNE2 show increased levels upon LNA inhibition of miR16, as they are targets of miR16-mediated repression (Liu et al., 2008). **iii.** Western blot of AGO2 IP from G0 cells. **iv.** FXR1-associated targets immunoprecipitate with AGO2 (shown 4 targets, Table S7). **E.** qRT-PCR analysis of endogenous target mRNA levels normalized to endogenous tRNA-lys in control and microRNA LNA inhibitor treated G0 cells. RNA levels do not decrease and do not account for the decrease in their protein levels upon LNA inhibition of their targeting microRNAs, as observed in Fig. 7C, Ei. Instead some targets show increase in total RNA levels upon microRNA inhibition, observed even with normalization to multiple different loading control RNAs. This may be due to indirect stabilization of the mRNAs upon loss of the translation of these mRNAs upon microRNA inhibition of their translation activation—as also observed upon inhibition of target mRNA translation activation due to loss of FXR1 and thereby FXR1a-microRNP mediated activation in FXR1 knockdown cells in Fig. S7C. **F.** qRT-PCR analysis of Luciferase reporter A0 mRNA levels (normalized to Renilla control mRNA) of reporters bearing: **i.** CD209 3′-UTR, reverse CD209 3′-UTR (REV), and with mutated miR16 target site (mtCD209 3′-UTR) and **ii.** HES1 3′-UTR and with mutated miR369-3p target site (mtHES1 3′-UTR) in G0 cells. RNA levels do not change significantly and do not reflect the translation in Fig. 7Di-ii (CD209 reporters) and Fig. 7Eii-iii (HES1 reporters). **G.** qRT-PCR analysis upon p97 and PARN knockdown in G0 cells, of samples: **i.** from Fig. 7Fi, endogenous candidate target mRNAs, normalized to endogenous tRNA-lys (endogenous TNFα mRNA levels monitored in Fig. S3C (PARN knockdown) and Fig. S4B (p97 knockdown)), and **ii.** from Fig. 7Fii, of the CD209 3′-UTR and reverse CD209 3′-UTR (REV) bearing Luciferase reporter A0 mRNA levels, normalized to Renilla control mRNA. RNA levels in these control and knockdown cells do not change significantly and do not reflect the translation changes observed in

Fig. 7Fi-ii. **H.** In proliferating cells and mature oocytes, mTOR activity is high, leading to phosphorylation and inactivation of the canonical cap-dependent translation inhibitor, 4EBP. This permits canonical translation to proceed where the cap-binding protein, eIF4E, can bind eIF4G, which further reinforces cap association by this complex, and via eIF4G association with PABP, connects the 5′ and 3′ ends of the mRNA to promote translation (Sonenberg and Hinnebusch, 2009). In immature oocytes and G0 cells, where mTOR activity is low, 4EBP is hypophosphorylated (Fig.6A, S6D), enabling 4EBP to inhibit eIF4E-eIF4G interaction and thereby, decrease canonical translation in these conditions (Loayza-Puch et al., 2013; Thoreen et al., 2012; Hsu et al., 2011; Seal et al., 2005; Radford et al., 2008; Thoreen et al., 2009). Non-canonical, cap-independent translation mechanisms can function in these conditions to enable the translation of specific mRNAs. Our data suggest that FXR1a-microRNP mediated translation activation may function as one such alternative mechanism that enables translation of recruited mRNAs. FXR1a does not associate with the microRNP repressor, GW182, in these cells (Fig. S5D-E), and instead promotes translation upon overexpression (Vasudevan and Steitz, 2007; Truesdell et al., 2012), or in conditions where FXR1 levels increase—including G0, Torin 1 treatment and immature oocyte stages (Fig. 6A, S6D). Consistent with these suppressed canonical translation conditions, targets of microRNA-mediated activation have shortened poly(A) tails (Fig. 1A, C, 3A-B, S1B, S3D) to avoid PABP (Fig. 1G-I, S5B-C)—as PABP would enhance microRNA-mediated inhibition via GW182 (Fabian et al., 2010; Beilharz et al., 2009; Moretti et al., 2012), and promote canonical cap and poly(A)-dependent translation that is reduced in these conditions by hypophosphorylated 4EBP (Fig. 6A, S6D). Poly(A) shortened mRNAs have been found to be present in human cells (Cheng et al., 2005; Meijer et al., 2007; Cui et al., 2010; Yang et al., 2011). Specific unadenylated mRNAs can be translated (Wang and Wang, 2015; Jopling et al., 2005; Roberts et al., 2011; Ling et al., 2002; Smith and Gray, 2010; Wilusz et al., 2012; Marzluff et al., 2008; Yanagiya et al., 2010), and the poly(A) tail has been

shown to not correlate with translation efficiency in distinct stages (Subtelny et al., 2014), consistent with our findings of microRNA-mediated translation activation of poly(A) shortened target mRNAs. FXR1a-microRNP can bind the 3′-UTR microRNA target site of these specific mRNAs—selectively recruited in the nucleus (Truesdell et al., 2012)—and interacts with the eIF4G paralog , p97 (Fig. 4B), while PARN associates increasingly with the 5′ cap of mRNAs in G0 (Seal et al., 2005) (Fig. 5B), and PARN can also directly or indirectly interact with FXR1a and p97 (Fig. 5E). This suggests the formation of an alternate complex where the 5′ cap-bound PARN can connect p97 that is associated with the 3′-UTR bound FXR1a-microRNP, to the 5′ end. P97 can interact with eIF3 and thereby, recruit the 40S ribosome subunit to initiate non-canonical translation (Lee and McCormick, 2006; Levy-Strumpf et al., 1997; Ramirez-Valle et al., 2008) (Baker and Fuller, 2007; Nousch et al., 2007; Nevins et al., 2003), specifically of the recruited mRNAs in these reduced canonical translation conditions. FXR1 was also shown to interact with 60S ribosome subunit factors (Siomi et al., 1996) and could also promote activation via these interactions. PARN also interacts with AGO2 (Zhang et al., 2015), supporting a role for PARN with FXR1a-microRNP. Specific mRNAs are selected for activation as FXR1a-microRNP recruits its targets selectively in the nucleus (Truesdell et al., 2012), which are then subject to this non-canonical translation mechanism for specific mRNA expression in these conditions of reduced canonical translation. MicroRNA target mRNAs that are not recruited by FXR1a-microRNP in the nucleus (Truesdell et al., 2012), are not directed for activation; these targets may be recruited in the cytoplasm (Weinmann et al., 2009) by GW182-microRNPs, and are repressed and downregulated.

Supplemental Tables Legends (Tables S1-S5, S7 are excel files)

Table S1, Related to Fig. 1-7, S1-S7 Global proteomic analysis/TMT mass spectrophotometry analysis of 3 biological replicates of THP1 cells with and without FXR1 knockdown in G0 THP1 cells

Sheet 1: Combined 3 sets of mass spectrometry analysis

Sheet 2: Protein candidates with ≥1.5 fold decrease (log2FC≤-0.585, log2FC in column S) in FXR1 knockdown compared to control shRNA cells (selected activation target of miR16 marked in teal)

Sheet 3: Protein candidates with significant decrease ($p \leq 0.05$, p value in column T)

Sheet 4: Protein candidates based on both fold change (≥1.5 fold decrease, log2FC≤-0.585, log2FC in column S) and statistical significance ($p \leq 0.05$, p value in column T) in FXR1 knockdown compared to control shRNA cells (candidate activation targets of miR16 and miR369-3p are marked in teal)

Table S2, Related to Fig. 1-7, S1-S7 Combined mass spectrometry analysis normalized for RNA levels from total RNA samples of FXR1 knockdown compared to control shRNA cells.

Mass spectrometry analysis normalized for total RNA levels (RNA levels measured by microarray), referred to as TE, to check that selected mass spectrometry candidates (identified from Table S1) are affected at the protein level beyond effects at the RNA level—at ≥ 1.45 fold decrease upon FXR1 knockdown in TE or mass spectrometry protein levels normalized for RNA levels (Table S2, Column V for TE or mass spectrometry protein levels normalized for RNA levels; selected candidate activation targets marked in teal). All of the targets tested were validated by qRT-PCR of total RNA levels (Fig. S7C) to check that the decrease in target protein levels (Table S1) do not correlate with their total RNA levels, indicating that the change in protein levels is not due to changes in RNA levels.

Table S3, Related to Fig. 1-7, S1-S7 Results of functional enrichment analysis among proteins identified by mass spectrometry

Sheet 1: DAVID analysis of protein set with significant change ($p \leq 0.05$)

Sheet 2: DAVID analysis of protein set with ≥ 1.5 fold decrease in FXR1 knockdown compared to control shRNA cells; Graph in Fig. S7Aii enlarged

Table S4, Related to Fig. 1-7, S1-S7 Predicted miR16 targets of activation from global mass spectrometry analysis

Sheet 1: Predicted sites for all—upregulated, downregulated (potential activation targets) and unchanged upon FXR1 knockdown—miR16 candidate targets (activation and repression) in THP1 G0 (predicted by Mirror (Friedman and Linial, 2013) and Targetscan (Friedman et al., 2009)) present in all 3 replicates of the mass spectrometry data. Targets that are downregulated upon FXR1 knockdown require FXR1 for their expression and are potential activation targets. Targets that are upregulated or unchanged upon FXR1 knockdown are not activation targets and are regulated by other processes.

Sheet 2: miR16 targets upregulated upon FXR1 knockdown; 23 genes with $p \leq 0.05$ (p value in column AL). The cutoff ($p \leq 0.05$) is marked in green.

Sheet 3: miR16 targets downregulated upon FXR1 knockdown; 3 genes with $p \leq 0.05$ (p value in column AL) were detected as potential activation targets. The cutoff ($p \leq 0.05$) is marked in green.

Sheet 4: miR16 targets downregulated upon FXR1 knockdown based on fold change (≥1.5 fold decrease upon FXR1 knockdown, $log2FC \leq -0.585$, log2FC in column AK). 37 genes were detected as potential activation targets with ≥1.5 fold decrease ($log2FC \leq -0.585$) in FXR1 knockdown compared to control shRNA cells (tested targets marked in teal). The cutoff ($log2FC \leq -0.585$) is marked in green.

Sheet 5: miR16 targets downregulated upon FXR1 knockdown in the subset with $p \leq 0.05$ (column AL) and ≥1.5 fold decrease ($log2FC \leq -0.585$, log2FC in column AK) in FXR1 knockdown compared to control shRNA cells. The cutoff ($p \leq 0.05$ and $log2FC \leq -0.585$) is marked in green. 3 activation targets were detected (tested targets marked in teal).

Sheet 6: miR16 targets downregulated upon FXR1 knockdown shown in Fig. S7B.

Table S5, Related to Fig. 1-7, S1-S7 Predicted miR369-3p targets of activation from global mass spectrometry analysis

Sheet 1: Predicted sites for all—upregulated, downregulated (potential activation targets) and unchanged upon FXR1 knockdown—miR369-3p candidate targets (activation and repression) in THP1 G0 (predicted by Mirror (Friedman and Linial, 2013) and Targetscan (Friedman et al., 2009)) present in all 3 replicates of the mass spectrometry data. Targets that are downregulated upon FXR1 knockdown require FXR1 for their expression and are potential activation targets. Targets that are upregulated or unchanged upon FXR1 knockdown are not activation targets and are regulated by other processes.

Sheet 2: miR369-3p targets upregulated upon FXR1 knockdown; 3 genes with $p \leq 0.05$ (p value in column AJ). The cutoff ($p \leq 0.05$) is marked in green.

Sheet 3: miR369-3p targets downregulated upon FXR1 knockdown; 3 genes with $p \leq 0.05$ (p value in column AJ) were detected as potential activation targets. The cutoff ($p \leq 0.05$) is marked in green.

Sheet 4: miR369-3p targets downregulated upon FXR1 knockdown based on fold change (≥1.5 fold decrease upon FXR1 knockdown, $log2FC \leq -0.585$, log2FC in column AI). 5 genes were detected as potential activation targets with ≥1.5 fold decrease ($log2FC \leq -0.585$) in FXR1 knockdown compared to control shRNA cells (tested targets marked in teal). The cutoff ($log2FC \leq -0.585$) is marked in green.

Sheet 5: miR369-3p targets downregulated upon FXR1 knockdown in the subset with $p \leq 0.05$ (p value in column AJ) and ≥1.5 fold decrease ($log2FC \leq -0.585$, log2FC in column AI) in FXR1 knockdown compared to control shRNA cells. The cutoff ($p \leq 0.05$ and $log2FC \leq -0.585$) is marked in green. 3 activation targets were detected (tested targets marked in teal).

Sheet 6: miR369-3p targets downregulated upon FXR1 knockdown shown in Fig. S7B.

Table S6, Related to Fig. 1-7, S1-S7 Primer list

Table S7, Related to Fig. 1-7, S1-S7 Table of targets tested

Table S6

TNFα (360-5′) Forward	5'-CCCAGGGACCTCTCTCTAATCA-3'
TNFα (470-3′) Reverse	5'-AGCTGCCCCTCAGCTTGAG-3'
CD209 Forward	5'- CTG CAG TGG AAC GCC TGT -3'
CD209 Reverse	5'- CTG TAG GAA GTT CTG CTC CTC AG -3'
FEZ1 Forward	5'- CCT CTC CGA GCT TGA GAA TTT TTC -3'
FEZ1 Reverse	5'- GGA TCT GTA ACT GGT TCT TCA C -3'
NUAK1 Forward	5'- GAG GGC CAG AGG TGG ACA -3'
NUAK1 Reverse	5'- CTC GAG CAT CTG AGG GCT G -3'
TOM1L1 Forward	5'- GGC CAC CTC ATA GAA AAG GCT AC -3'
TOM1L1 Reverse	5'- GCT TTC ACT GCA TCT TTT GGC C -3'
TOM1L1 Forward2	5'- CCT TGT CAC TTA TTG ACA TGT GTG -3' used for FXR1 immunoprecipitates
TOM1L1 Reverse2	5'- CTA ATG GCA AGT TGT ATC TGG G -3' used for FXR1 immunoprecipitates
NARG2 Forward	5'- CAG GAC TGA ATT GGG ATA TTT CC -3'
NARG2 Reverse	5'- CGT CTG TTG GAT AAA ACA CGT AG -3'
HES1 Forward 1001	5'- GAC TCC ATG TGG AGG CCG TG -3'
HES1 Reverse 1220	5'- ATA TAG TGC ATG GTC AGT CAC -3'
CD93 Forward	5'- CTA CAT CCT AGG CAC CGT GGT G -3'
CD93 Reverse	5'- GAG TAA CTG TCT GCC GCA TTC -3'
CCND3 Forward	5'- GTG CTA CAG ATT ATA CCT TTG CC -3'
CCND3 Reverse	5'- CAG GCA GTC CAC TTC AGT G -3'
CCNE2 Forward	5'- GCC TGA TTT AAG CTG GGG ATG -3'
CCNE2 Reverse	5'- CCA GTC TAG AAG TAT GGA CCT C -3'
TRPS1 Forward	5'- GAT GTG CAG GTG ACT TCA GGT G -3'
TRPS1 Reverse	5'- CTA ATT CGG TGG ATG AGT TGC CC -3'
tRNA-Lys Forward	5'- GCCCGGATAGCTCAGTCGGTAGAG-3'
tRNA-Lys Reverse	5'- CGCCCGAACAGGGACTTGAACCC-3'
xl-tRNA-Lys Forward	5'-CCCGCATAGCTCAGTCGGTAGAGC-3'
xl-tRNA-Lys Reverse	5'-CCCGAACAGGGACTTGAACCC-3'
hs-beta Actin Forward	5'-ATTGGCAATGAGCGGTTC-3'
hs-beta Actin Reverse	5'-CGTGGATGCCACAGGACT-3'
Firefly Forward (F10-5)	5'-GGATTACGTGGCCAGTCAAGTAACAACCG-3'
Firefly Reverse (7F3-Rev)	5'-GGATCTCTCTGATTTTTCTTGCGTCGAG-3'
Firefly Forward (FF-F3)	5'-TTCCATCTTCCAGGGATACG-3'
Firefly Reverse (FF-R3)	5'-ATCCAGATCCACAACCTTCG-3'
Renilla (Ren1) Forward	5'-CCATGATAATGTTGGACGAC-3'

Renilla (Ren2) Reverse	5'-GGCACCTTCAACAATAGCATTG-3'
CD209-NotI FWD	5'- gactGCGGCCGCGCT ACA GTT CCT TCT CTC C -3' CD2093'UTR 1282-1770 miR-16 region
CD209-NotI REV	5'- CAGTGCG GCC GC CTC TGG GTG CCA TTG GTT -3' CD2093'UTR 1282-1770 miR-16 region
CD209-miR16-SDM FWD **mutant** miR16 site	5'- GGT TGC CAT GTG TAG **A**TG **T**TA TGT CCC CTG G -3'
CD209-miR16-SDM REV **mutant** miR16 site	5'- CCA GGG GAC ATA ACA **T**CT **A**CA CAT GGC AAC C -3'
mutPARN-W468A Forward	5'- GGT AAC ATT CAG ATA TCC **GC**C ATT GAT GAT -3'
mutPARN-W468A Reverse	5'- ATC ATC AAT **GG**C GGA TAT CTG AAT GTT ACC -3'
MYT3245-5 Forward	5'-CAGTATTGTTGAATATATCATGTAACC-3'
MYT3245 -3 Reverse	5'-CTGCCATTATCAAGCAGGAGCACTGC-3'
HES1 UTR Fwd (NotI)	5'-AAGGAAAAAAGCGGCCGCgggggctcaggccacccctc ctcctaaactccc-3'
HES1 UTR Rev (NotI)	5'-AAGGAAAAAAGCGGCCGCattttctcaaataaacttccccaaaggaag-3'
HES1miR369p**mut** FW	5′-catattggattgcgcctttt**gtaCCata**aaagctcagatgacatttcg-3′

SI Extended Procedures

Identification of activation targets

Proteomic analysis in FXR1 knockdown cells Proteomic analysis has been used previously for microRNA target identification (Baek et al., 2008; Selbach et al., 2008). To identify targets of activation, we conducted multiplex proteomic analysis, by Tandem-Mass Tag (TMT) mass spectrometry (Ting et al., 2011) (Table S1) in G0 cells with and without FXR1 depletion. FXR1 knockdown was used in order to globally identify activation targets of more than one microRNA, since FXR1 is required for microRNA-mediated activation by FXR1a-microRNP in G0 (Vasudevan et al., 2007), and does not associate with repressive GW182-microRNPs in these cells (Fig. S5D-E). Doxycycline-inducible FXR1 shRNA and control shRNA stable THP1 cells were induced with 1 μg/ml of doxycycline continually to cause knockdown of FXR1 (Fig. 7Ai): the cells were grown in serum for 3 days to express the shRNAs, followed by 2 days of serum-starvation to enter G0. 3 biological replicates of FXR1 knockdown and control shRNA G0 cells were subject to TMT mass spectrometry analysis as described in the below section on proteomic analysis (Ting et al., 2011). Gene Ontology (GO) analysis for differentially expressed genes (Fig. S7Aii, Table S3) was performed with the DAVID tool (Huang et al., 2008), which revealed enrichment of immune genes (such as CD209, which we validated as a miR16 activation target in Fig. 7, S7), RNA binding genes and other categories.

Target identification Our data revealed that miR16 and miR369-3p associate with FXR1 (Fig. 7Biii), indicating a potential role for these microRNAs in activation. The top miR16 and miR369-3p targets that are downregulated in FXR1 knockdown G0 cells compared to control shRNA G0 cells—targets that require FXR1 for upregulation—were identified. MicroRNA target identification was conducted using MiRror and TargetScan (MiRror combines analysis of several target site identification tools (Friedman et

al., 2009; Friedman and Linial, 2013)). Targets were identified from genes from the mass spectrometry data as well as from G0-expressed candidate targets (targets known to be expressed in G0) that are downregulated upon FXR1 knockdown. Overall, from the 7083 genes from the 3 replicates of the mass spectrometry data, we found 1445 miR16 and 51 miR369-3p predicted target site bearing genes using MiRror and TargetScan analyses. These include downregulated genes that are potential activation targets as they are decreased upon FXR1 depletion (and therefore, require FXR1 for their expression)—as well as unchanged and upregulated genes. The unchanged and upregulated genes could be regulated by other processes or are likely repression targets, as they harbor microRNA target sites; since these genes are not decreased upon FXR1 depletion, they are therefore, not targets of activation by FXR1a-microRNP in THP1 G0 cells. Targets of microRNA-mediated activation were screened and tested from the following 3 categories:

a. Targets downregulated upon FXR1 knockdown based on fold change (≥1.5 fold decrease upon FXR1 knockdown) Tables S4-5, sheet 4

From the mass spectrometry data of 3 biological replicates with 7083 common genes, protein candidates with ≥1.5 fold decrease (log2FC≤-0.585, log2FC in column S, Table S1, sheet 2) in FXR1 knockdown compared to control shRNA cells (requires FXR1 for expression and are therefore, potential activation targets), consisting of 230 genes (Table S1, sheet 2), were screened for target sites for the two FXR1-associated microRNAs, miR16 and miR369-3p. Based on fold change of ≥1.5 fold decrease (log2FC≤-0.585, log2FC in column S, Table S1, sheet 2) in FXR1 knockdown compared to control knockdown cells, 37 miR16 targets (Table S4, sheet 4, ≥1.5 fold decrease or log2FC≤-0.585, log2FC in column AK) and 5 miR369-3p targets (Table S5, sheet 4, ≥1.5 fold decrease or log2FC≤-0.585, log2FC in column AI) of activation were identified, some of which were further validated (Fig. 7, S7, Table S7). These included

targets such as FEZ1 (marked in teal in Table S1, sheet 2; also in Table S4, sheet 4; Table S7) that were further validated (Fig. 7, S7).

b. Targets downregulated upon FXR1 knockdown based on statistical significance (p≤0.05) and fold change (≥1.5 fold decrease) upon FXR1 knockdown Tables S4-5, sheet 5

From the mass spectrometry data of all 3 biological replicates, protein candidates with significant decrease (p≤0.05, Table S1, sheet 3, p value in column T), consisting of 125 genes (Table S1, sheet 3), were screened for target sites of miR16 and miR369-3p (Tables S4-S5; Table S7). This yielded 26 miR16 target genes (23 upregulated genes (Table S4 sheet 2, p≤0.05, p value in column AL) + 3 downregulated genes (Table S4 sheet 3, p≤0.05, p value in column AL)) and 6 miR369-3p target genes (3 upregulated genes (Table S5 sheet 2, p≤0.05, p value in column AJ) + 3 downregulated genes (Table S5 sheet 3, p≤0.05, p value in column AJ)). These include downregulated genes that are potential activation targets, as they are decreased upon FXR1 depletion—as well as genes that are not decreased upon FXR1 depletion, which are potentially controlled by other processes.

Protein candidates, decreased in FXR1 knockdown compared to control shRNA cells, based on both fold change (≥1.5 fold decrease upon FXR1 knockdown, log2FC≤-0.585, Table S1, sheet 4, log2FC in column S), and statistical significance (p≤0.05, Table S1, sheet 4, p value in column T), are potential activation targets. 8 common genes among the 125 genes (p≤0.05, Table S1, sheet 3, p value in column T) also show a fold change of ≥1.5 fold decrease in FXR1 knockdown compared to control knockdown cells and are therefore, dependent on FXR1 for expression, and are potential activation targets (shown in Table S1, sheet 4, ≥1.5 fold decrease upon FXR1 knockdown, log2FC≤-0.585, log2FC in column S and p≤0.05, p value in column T). These include targets of miR16 (Table S4, sheet 5, p≤0.05, p value in

column AL and ≥1.5 fold decrease or log2FC≤-0.585, log2FC in column AK) and miR369-3p (Table S5, sheet 5, p≤0.05, p value in column AJ and ≥1.5 fold decrease or log2FC≤-0.585, log2FC in column AI) such as CD209, TOM1L1 and NARG2 (Table S1, sheet 4, marked in teal; Tables S4-S5, sheet 5; Table S7) that were further validated (Fig. 7, S7).

c. G0-expressed candidate targets Additional candidate targets associated with known expression in G0/cell cycle arrest—TNFα (Vasudevan et al., 2007), HES1 (Coller et al., 2006; Sang et al., 2008), and NUAK1 (Sun et al., 2013)—that are either secreted (TNFα cytokine) and thereby, not analyzed as the mass spectrometry analysis excluded extracellular media, or are not resolved by mass spectrometry that is limited to ~8000 genes, were screened for target sites and validated similarly (Table S7, Fig. 7, S7).

Additional Screens & Validation

1. Mass spectrometry data proteomic changes upon FXR1 knockdown could be due to translation or protein stability, or RNA levels. First, to check for regulation at the translation level by FXR1, the above candidates were tested for their requirement for FXR1 for polysome association of their target mRNAs. This was done by qRT-PCR analysis of polysome associated mRNAs, where potential activation targets show decreased association with polysomes in FXR1 knockdown cells compared to control shRNA cells (Fig. 7Aii-iii), without concurrent decrease in total RNA levels (Fig. S7C). Since proteomic data changes could also be due to changes at the RNA level, the mass spectrometry data of common genes in all 3 biological replicates were further normalized for fold change in total RNA levels (Table S2, RNA levels were detected by microarrays of total RNA from FXR1 knockdown compared to control shRNA cells). This is similar to the previously defined translation efficiency/TE with Luciferase protein activity normalized to RNA levels to provide the protein output per RNA molecule (Wu et al., 2006; Vasudevan

and Steitz, 2007). In this case, mass spectrometry data instead of Luciferase activity read out the protein levels and is normalized for RNA levels. Genes decreased in FXR1 knockdown compared to control knockdown cells in the mass spectrometry data normalized for RNA are dependent on FXR1 for expression at the protein level beyond changes at the RNA level. The genes in this Table (Table S2) with ≥1.45 fold decrease upon FXR1 knockdown in the TE or mass spectrometry protein levels normalized for RNA (Table S2, Column V for the TE or mass spectrometry protein levels normalized for RNA), include the top targets from the above categories such as CD209, FEZ1 and NARG2 (Table S2, targets marked in teal). All the targets tested in this study, including these, were validated by qRT-PCR of total RNA levels in FXR1 knockdown and control shRNA knockdown cells, to ensure that their decreased association with polysomes upon FXR1 knockdown (Fig. 7Aii-iii), and decreased target protein levels in FXR1 knockdown cells (Table S1, S4-S5), is not due to a concurrent decrease in total RNA levels (Fig. S7C). These targets are affected at the protein level after normalization for RNA levels, and in conjunction with their requirement for FXR1 for polysome association (Fig. 7Aiii), indicate that FXR1 mediates their translation.

2. Second, to rule out candidates that are not associated with FXR1 and are indirectly regulated, these target mRNAs were tested by FXR1 co-immunoprecipitation analysis to validate their association with FXR1(Fig. 7Bi-ii). These targets were also tested for AGO2 association to validate that they are microRNP targets and thereby, FXR1a-microRNP associated targets (Fig. S7Diii-iv, 4 targets shown, Table S7). Candidates such as CCND3 and CCNE2 mRNAs that are not affected by FXR1 knockdown (Tables S1, S4, S7)—and therefore, are not targets of activation, and are negative controls—consistently, do not show significant association with FXR1 (Fig. S7Di).

3. Third, after verification through the above screens, the candidates were validated as functional targets of microRNA-mediated activation and of the identified p97 and PARN mechanism. The requirement for these microRNAs and these factors for target mRNA translation was demonstrated using LNA inhibitors against the microRNAs, p97 and PARN shRNA, with activation monitored by target 3′-UTR Luciferase reporters, endogenous protein and RNA levels (Table S7, Fig. 7C-F, S7E-G).

Activation targets Selective mRNA recruitment by FXR1 (occurs in the nucleus (Truesdell et al., 2012)) is essential for activation in G0 and discriminates between activation and repression, as FXR1associates with AGO2 and microRNAs (Vasudevan et al., 2007) but does not associate with repressive GW182 microRNPs in these cells (Fig. S5D-E). Therefore, microRNA target mRNAs that are not recruited by FXR1a-microRNP are not activation targets in THP1 G0 cells. We verified new miR16 targets (CD209, FEZ1, NUAK1), and new miR369-3p targets (HES1, NARG2, TOM1L1) through multiple assays (Fig. 7, S7), as well as tested previously identified targets of activation (MYT1 in oocytes, TNFα in THP1 cells). We also tested other targets and other microRNAs but did not find working antibodies for all targets (Table S7). The above validated (6 new and 2 previously identified) targets reveal microRNA-mediated activation with more than one microRNA, both of which are associated with FXR1 (Fig. 7Biii) and thereby, with FXR1a-microRNP.

Other targets identified (Tables S1, S4, S5) need to be screened and validated to be activation targets, as conducted above, as the presence of target sites and protein decrease upon FXR1 knockdown is not sufficiently conclusive, since microRNA target sites may not be used, may be cell line specific, and indirect processes may be involved as previously shown (Kedde et al., 2007; Bhattacharyya et al., 2006). Therefore, these numbers are an approximation. From the 7083 genes from the 3 replicates of the mass spectrometry data, using MiRror and TargetScan analyses, we found 1445 miR16 (Table S4) and 51

miR369-3p (Table S5) target site bearing genes. Applying a cutoff based on statistical significance of $p \leq 0.05$ yielded 26 miR16 target genes (23 upregulated genes (Table S4 sheet 2, $p \leq 0.05$, p value in column AL) + 3 downregulated genes (Table S4 sheet 3, $p \leq 0.05$, p value in column AL)) and 6 miR369-3p target genes (3 upregulated genes (Table S5 sheet 2, $p \leq 0.05$, p value in column AJ) + 3 downregulated genes (Table S5 sheet 3, $p \leq 0.05$, p value in column AJ)). These include genes that are downregulated (potential activation targets) upon FXR1 knockdown, and those that are upregulated/targets that are not decreased upon FXR1 depletion and are likely regulated by other processes. This subset ($p \leq 0.05$) was sorted based on fold change of ≥1.5 fold decrease in FXR1 knockdown compared to control knockdown cells; such genes require FXR1for their expression and are candidate activation targets. 3 miR16 activation targets (Table S4, sheet 5, $p \leq 0.05$, p value in column AL and ≥1.5 fold decrease upon FXR1 knockdown or log2FC≤-0.585, log2FC in column AK) out of 26 potential miR16 (activation targets and targets that are not decreased upon FXR1 depletion) targets, and 3 miR369-3p activation targets (Table S5, sheet 5, $p \leq 0.05$, p value in column AJ and ≥1.5 fold decrease upon FXR1 knockdown or log2FC≤-0.585, log2FC in column AI) out of 6 potential miR369-3p (activation targets and targets that are not decreased upon FXR1 depletion) targets were identified as candidate activation targets as they are downregulated ≥1.5 fold upon FXR1 knockdown. The candidates show consistent decrease in polysome association upon FXR1 knockdown as observed by qRT-PCR analysis of polysome associated mRNAs (Fig. 7Aiii, Table S7), without concurrent decrease in total RNA levels (Fig. S7C). These values are an estimate and would vary with target identification program, identifying polysome association, and direct versus indirect targets, as tested in Fig. 7A-B, as well as due to variabilities in mass spectrometry/ profiling analyses and immunoprecipitation efficiencies.

The mass spectrometry analysis excluded extracellular material and other factors due to limited resolution and was a restricted dataset (~7083 genes), indicating that the number of activation targets in

G0 could be higher compared to this limited dataset. Consistently, a few previously identified, G0-expressed candidate targets (Table S7)—TNFα, a cytokine that is secreted and therefore not present in the mass spectrometry data that excluded extracellular media, as well as HES1 and NUAK1—were found to require FXR1 for polysome association (Fig. 7Aiii), as they show a significant decrease in polysome association in FXR1 knockdown cells compared to control shRNA cells, without concurrently decreasing RNA levels (Fig. S7C). These candidates were subsequently validated as targets of activation (Fig. 7, S7).

Activation and repression Our previous data suggest that targets that are recruited by the FXR1a-microRNP (in the nucleus, (Truesdell et al., 2012)) are directed for activation—while other microRNA target mRNAs that are not recruited by FXR1a-microRNP, could be recruited and subject to repression by the canonical microRNP associated with GW182 (recruited in the cytoplasm (Weinmann et al., 2009)), which does not interact with FXR1 in these cells (Fig. S5D-E). We found that CCND3 and CCNE2, which are known to be decreased in G0 for maintenance of cell cycle arrest and are repressed by miR16 (Liu et al., 2008), are not affected by FXR1 knockdown (Tables S1, S4, S7), and are not associated with FXR1 (Fig. S7Di)—and therefore, are not targets of activation. Consistently, miR16 inhibition, with an LNA inhibitor, increased CCND3 and CCNE2 levels due to loss of repression (Fig. S7Dii), and CCND3 and CCNE2 are not decreased by depletion of factors required for activation; FXR1 (Tables S1, S4), p97 or PARN (Fig. 7Fi). Further global investigation of FXR1a-microRNP associated RNAs is needed and will categorize microRNAs recruited to FXR1a-microRNP as well as activation and repression targets.

Proteomic analysis Doxycycline-inducible FXR1 shRNA and control shRNA stable THP1 cells were induced with 1 μg/ml of doxycycline continually to cause knockdown of FXR1 (Fig. 7Ai); the cells were

grown in serum for 3 days to induce the shRNAs, followed by 2 days of serum-starvation to induce G0. $10x10^6$ cells per sample were pelleted and subject to Tandem Mass Tag (TMT) mass spectrometry analysis as previously described (Ting et al., 2011). 3 biological replicates were compared.

RNA analyses Total RNA from total cell lysates was harvested and analyzed by qRT-PCR (Fig. S7C). The mass spectrometry data comparing FXR1 knockdown and control shRNA cells was also normalized to microarray analysis of total RNA levels (Table S2), to obtain the normalized protein levels per RNA molecule, similar to the previously conducted translation efficiency/TE (Vasudevan and Steitz, 2007; Wu et al., 2006). Synthesized cDNA probe by WT Expression Kit (Ambion) was hybridized to Gene Chip Human Transcriptome Array 2.0 (Affymetrix) by the Partners Healthcare Center for Personalized Genetic Medicine Microarray facility (Lee et al., 2014).

Quantitative Proteomics Cell pellets were lysed in a buffer containing 75 mM NaCL, 50 mM HEPES (pH 8.5), 10 mM sodium pyrophosphate, 10 mM NaF, 10 mM β-glycerophosphate, 10 mM sodium orthovanadate, 10 mM phenylmethanesulfonylfluoride, Roche Complete Protease Inhibitor EDTA-free tablets, and 3 % sodium dodecyl sulfate. Lysis was achieved by passing cells 10 times through a 21-gauge needle. Lysates were further processed through reduction and thiol alkylation was followed by purifying the proteins using MeOH/CHCl3 precipitation. Protein digestion was performed with Lys-C and trypsin. Peptides were labeled with TMT-10plex reagents (Thermo Scientific) (McAlister et al., 2012) and fractionated by basic pH reversed phase chromatography as described elsewhere (Tolonen and Haas, 2014). Multiplexed quantitative proteomics was performed on an Orbitrap Fusion mass spectrometer (Thermo Scientific) using a Simultaneous Precursor Selection (SPS) based MS3 method (McAlister et al., 2014). MS2 spectra were assigned using a SEQUEST-based (Eng et al., 1994) proteomics analysis platform (Huttlin et al., 2010). Based on the target-decoy database search strategy (Elias and Gygi, 2007) and employing linear discriminant analysis and posterior error histogram sorting,

peptide and protein assignments were filtered to false discovery rate (FDR) of < 1 % (Huttlin et al., 2010). Peptides with sequences that were contained in more than one protein sequence from the UniProt database were assigned to the protein with most matching peptides (Huttlin et al., 2010). TMT reporter ion intensities were extracted as that of the most intense ion within a 0.03 Th window around the predicted reporter ion intensities in the collected MS3 spectra. Only MS3 with an average signal-to-noise value of larger than 40 per reporter ion as well as with an isolation specificity (Ting et al., 2011) of larger than 0.75 were considered for quantification. A two-step normalization of the protein TMT-intensities was performed by first normalizing the protein intensities over all acquired TMT channels for each protein based to the median average protein intensity calculated for all proteins. To correct for slight mixing errors of the peptide mixture from each sample a median of the normalized intensities was calculated from all protein intensities in each TMT channel and the protein intensities were normalized to the median value of these median intensities.

Oocytes Oocytes (immature, folliculated stages I-VI oocytes, defolliculated and matured oocytes) were manipulated as described previously (Moon et al., 2006). Injections were performed with immature, folliculated stage IV-VI oocytes (primarily stage IV oocytes) using Drummond Nanojet II system with volumes of 18 nl for reporters, RNAs and plasmids. 0.125 ng of GFP or PAIP2 expressing CMV plasmids were injected, or 0.125 ng of GFP or human p97, human eIF4G3, mouse PARN, and PARN mutants, expressing CMV plasmids or 10 ng of their transcribed RNAs/oocyte (Mortensen et al., 2011), were injected into the nucleus along with 37.5 ng of control (CCCAGGGACCTCTCTCTAATCA), or p97 antisense (CACTCTTGGTCTTCTGTTTCTTCCC), or PARN antisense (CTTAAAATTGCTCCTGGTGATTTCCATC). All antisense oligonucleotides were DNA, which at the concentrations used have been demonstrated to be effective (Peculis and Steitz, 1993; Prives and Foukai,

1991). The antisense targeted the ATG region (Mortensen et al., 2011). After incubation for 6-7 hr, 18 nl containing either ~0.5 ng and 0.1 ng DNA CMV plasmids expressing Firefly Luciferase and Renilla reporters were injected into the nucleus/oocyte (for plasmid expressed reporter assays), or 0.1 fmol (also 0.01 fmol) of each in vitro transcribed Luciferase reporter RNA was injected into the nucleus/oocyte (for RNA reporter assays). Translation was assayed after 3:30 hr and was conducted with folliculated stage IV oocytes (Truesdell et al., 2012). Analysis of maturation by scoring for Germinal Vesicle Breakdown (GVBD) was conducted with 20 oocytes for each sample (Mortensen et al., 2011).

Plasmids and Transfections pGIPZ constructs against human PARN, P97 and pTRIPZ vector control and CMV-SPORT6 plasmids encoding mouse PARN, PAIP2 and human p97 or eIF4G3 used were obtained from Open Biosystems/GE healthcare Dharmacon. HA-PAIP2 and 4EBP constructs were from A. Yanagiya & N. Sonenberg (Karim et al., 2006). All other plasmids, reporters and microRNAs used were previously described (Truesdell et al., 2012; Vasudevan et al., 2008). TNFα 3′-UTR Firefly Luciferase reporter used as an A0 mRNA is the TNFα ARE reporter bearing the ARE region with miR369-3p target sites (Vasudevan and Steitz, 2007). 3′-UTR reporters were constructed as described previously, cloning the entire 3′-UTR of HES1 (bearing the miR369-3p site) and of the 3′-UTR 1282-1770 (bearing the miR-16 target site) of CD209 into the NotI site of the CX Luciferase reporter plasmid (Vasudevan and Steitz, 2007). Mutated target sites and PARN mutants were created by Quikchange (Stratagene). Primers are described in Table S6. Stable THP1 cell lines were created using doxycycline inducible FXR1 shRNA and pTRIPZ lentiviral vector (Open Biosystems/GE healthcare Dharmacon), and were induced at 1 μg/ml of doxycycline continually to cause knockdown of FXR1 (Fig. 7Ai); the cells were grown in serum for 3 days to induce the shRNAs, followed by 2 days of serum-starvation to induce G0. Transient transfections were conducted using nucleofection (Lonza) in THP1 cells.

MicroRNA & LNA All microRNAs had a 5′ monophosphate on the guide microRNA strand, were designed, annealed, and introduced as double-stranded RNAs (Doench et al., 2003; Doench and Sharp, 2004) synthesized by Integrated DNA Technologies. MicroRNAs let-7a, miR369-3p and miRcxcr4 were described earlier (Doench et al., 2003; Doench and Sharp, 2004; Vasudevan et al., 2007; Vasudevan et al., 2008). Inducible pTRIPZ and pTMP vectors were used in some experiments to express control miR30 or miRcxcr4 (previously cloned into the vectors) (Truesdell et al., 2012; Vasudevan et al., 2008) by inducing with 1 μg/ml of 1 mg/ml (stock) doxycycline for 42 hr to 5 days, as described. LNA Power Inhibitors (Exiqon) were used against miR16, miR24 (as a control), miR369-3p and the cxcr4 sequence (as a control). LNAs were nucleofected (Lonza) at 50 nM and ~20% nucleofection/transfection efficiency—after titration analyses that revealed significant cell death in G0 at higher concentrations or higher nucleofection efficiencies (using the programs prescribed by the manufacturer, Lonza), and poor effects at lower concentrations due to low transfection/nucleofection efficiency of THP1 cells and increased cell death upon nucleofection in THP1 G0 cells. 50 nM with ~20% nucleofection efficiency equates to 10 nM, which is similar to the concentrations used in studies that developed key LNA inhibitors (Obad et al., 2011).

Poly(A) Tail Analysis (PAT) assays Ligated-PAT assay was tested as described (Rassa et al., 2000) using the P1 ligate primer (5′-P-GGTCACCTTGATCTGAAGC-NH2-3′, 5′-phosphorylated and 3′−blocked with an amino group), which was ligated by T4 RNA ligase to the RNA sample overnight in a 27 μl reaction at room temperature. This was followed by cDNA synthesis using P1APCR (5′-GCTTCAGATCAAGGTGACCT-3′) and the cDNA was subjected to touchdown PCR (95°C denaturation for 45 seconds, 20 cycles touchdown from 68°C to 48°C annealing for 30 seconds, 72°C extension for 30 seconds, 35-40 cycles of amplification at 48°C with 95°C denaturation for 45seconds,

48°C annealing for 30 seconds and 72°C extension for 30 seconds) using TNF3END5 (5′-CCCATGTAGCCCCCTGGCCTCTGTGCC-3′, 160 nt upstream of the 3′ end of TNFα mRNA) as the forward primer and P10PCR (5′-GCTTCAGATCAAGGTGACC-3′) primer as the reverse primer for TNFα mRNA poly(A) tail.

RACE-PAT was performed for Fig. 1C as described (Salles et al., 1999) for Myt1 mRNA using MYT3421 (5′-GCAGTGCTCC TGCTTGATAATGGCAG-3′) primer as forward primer and the dT18 primer as the reverse primer on cDNA prepared with dT18 primer from unligated RNA samples from 10 oocytes/sample and was analyzed by ethidium bromide staining of agarose gels.

A modified tailing PAT assay was used for all PAT figures except for the RACE-PAT in Fig. 1C (Bazzini et al., 2012; Chang et al., 2014; Kusov et al., 2001) to detect short and no poly(A) tail bearing mRNAs as well as polyadenylated mRNAs. The assay extends the 3′ end of mRNAs with short poly G or poly C tails using poly(A) polymerase (PAP). G/I and G tail addition with yeast PAP did not work well in our assays and may prefer a 3′ end with at least a few As, as previously observed with G/I tailing (Bazzini et al., 2012). PAP from E.coli (ePAP from Ambion and Epicentre), with CTP or GTP for 1.5-3 hr, works well with CTP and less efficiently with GTP to extend the 3′ end in our assays, as previously observed (Yehudai-Resheff and Schuster, 2000), and was used to detect short and no poly(A) tail bearing mRNAs as well as polyadenylated mRNAs. After tailing the RNA samples with PAP, RT-PCR assay was performed (Bazzini et al., 2012). The RNAs are reverse transcribed with an RT primer that can anneal with the extended tail. Using the RT primer sequence as the forward primer on the cDNA, as well as a gene specific primer (based on the 5′-3′ mRNA sequence to act as reverse primer on the cDNA), 100-200 nt upstream of the 3′ end, the 3′ end is amplified by PCR to produce a short form in the case of a control A0 mRNA, or extended forms in the case of a control poly(A) mRNA or in the absence of PARN. Universal 10C (Bazzini et al., 2012) was used as the RT primer

(GGTAATACGACTCACTATAGCGAGACCCCCCCCCC) after tailing with GTP and ePAP for 1.5-3 hr for assays with THP1 cells. Universal 5G (GGTAATACGACTCACTATAGCGAGAGGGGG) was used as the RT primer after tailing with CTP and ePAP for 1.5 hr for oocytes, as this appears to work with oocyte samples. After cDNA preparation, an RT sequence primer that acts as the forward primer (Universal 5G in the case of oocytes or Universal RT primer, GGTAATACGACTCACTATAGCGAG for either THP1 or oocytes since both RT primers bear this common sequence) along with gene specific primers (based on the 5′-3′ mRNA sequence) that act as the reverse primer on the cDNA, were used to amplify the 3′ ends of different target mRNAs. The gene specific primers (based on the 5′-3′ mRNA sequence to act as reverse primers with the RT sequence forward primer on the cDNA) are:

TNF3END5: CCCATGTAGCCCCCTGGCCTCTGTGCC;

MYT3421 GCAGTGCTCCTGCTTGATAATGGCAG;

FF3END5 GCCAAGAAGGGCGGAAAGTCCAAATTG;

CD209-3841: CCTTTTCGGGCGCAGCCATCTTGCC. The PCR reaction was set up with 1.5 mM $MgCl_2$, 0.5 mM dNTPs, 50 pmol gene specific reverse primer, 50 pmol appropriate RT sequence forward primer for the PCR, 5 µL of prepared cDNA, and ~1U *Taq* DNA Polymerase in a thermal cycler with 45°C annealing for 60 seconds and 72°C extension for 60 seconds for 40-45 cycles. The reaction was then run on a 3% agarose gel with Ethidium Bromide for imaging. In each case, control mRNAs with no poly(A) or A0, A5, A20, poly(A) or an RNA sample treated with oligo dT and RNase H (to remove the poly(A) tail) were also used for the tailing and RT-PCR based PAT assay, as size controls. The same test RNA samples were also subject to qRT-PCR analysis to ensure that the RNA levels were equivalent in each case.

Crosslinking, Immunoprecipitation and Western Analyses As described previously (Truesdell et al., 2012). Nuclear-cytoplasmic fractionation was performed and the two fractions combined—for total extracts for Western analysis, and for in vivo formaldehyde crosslinked immunoprecipitation samples. In vivo crosslinking was done to enable high stringency washes of the in vivo complexes (Vasudevan and Steitz, 2007) to prevent any re-assortment of proteins/RNAs and non-specific interactions during extract preparation, which is known to happen with some RNA binding proteins (Mili and Steitz, 2004; Riley et al., 2012) differentially (Penalva et al., 2004). The samples were treated with RNase A/T1 and Turbo DNase (Ambion), and pre-cleared with anti-myc agarose. Anti-p97 (Cell Signaling), anti-FXR1 (Y19 & C18 used together at 12.5 µl each, Santa Cruz), anti-AGO (2A8, Millipore (Nelson et al., 2007)), anti-PARN (H-105, Santa Cruz), and anti-PABP (10E10 (Dreyfuss et al., 1984), Santa Cruz) were used for immunoprecipitation. Blots were probed with anti-FXR1 (6BG10, Millipore (Siomi et al., 1996) and ab51970, Abcam), anti-PARN for human protein (a gift from E. Wahle (Dehlin et al., 2000)), anti-GW182/18033 antibody (a gift from M. Fritzler, (Yang et al., 2004; Yu et al., 2005)) anti-AGO2 (rabbit, Millipore); anti-Tubulin, anti-HES1 (Santa Cruz); anti-Actin (Sigma); anti-HA (Covance); anti-NUAK1, anti-FEZ1, anti-CD209 (ProteinTech); anti-TOM1L1 (Bethyl antibodies); anti-NARG2 (Bioss antibodies); anti-phospho-4EBP (pSer65/Thr70, Santa Cruz sc12884); anti-S6, anti-phospho-S6; anti-p97, anti-TNFα, 4EBP (53H11), anti-MYT1, anti-Histone H3 and anti-phospho-CDC2 (Cell Signaling). Anti-PARN for *Xenopus* PARN (a gift from M. Wormington (Korner et al., 1998)) was used for immunoneutralization in oocytes.

Reference List

Baek,D., Villen,J., Shin,C., Camargo,F.D., Gygi,S.P., and Bartel,D.P. (2008). The impact of microRNAs on protein output. Nature *455*, 64-71.

Baker,C.C. and Fuller,M.T. (2007). Translational control of meiotic cell cycle progression and spermatid differentiation in male germ cells by a novel eIF4G homolog. Development *134*, 2863-2869.

Bazzini,A.A., Lee,M.T., and Giraldez,A.J. (2012). Ribosome profiling shows that miR-430 reduces translation before causing mRNA decay in zebrafish. Science *336*, 233-237.

Beilharz,T.H., Humphreys,D.T., Clancy,J.L., Thermann,R., Martin,D.I., Hentze,M.W., and Preiss,T. (2009). microRNA-mediated messenger RNA deadenylation contributes to translational repression in mammalian cells. PLoS. One. *4*, e6783.

Bhattacharyya,S.N., Habermacher,R., Martine,U., Closs,E.I., and Filipowicz,W. (2006). Relief of microRNA-Mediated Translational Repression in Human Cells Subjected to Stress. Cell *125*, 1111-1124.

Chang,H., Lim,J., Ha,M., and Kim,V.N. (2014). TAIL-seq: genome-wide determination of poly(A) tail length and 3' end modifications. Mol. Cell. *53*, 1044-1052.

Cheng,J., Kapranov,P., Drenkow,J., Dike,S., Brubaker,S., Patel,S., Long,J., Stern,D., Tammana,H., Helt,G., Sementchenko,V., Piccolboni,A., Bekiranov,S., Bailey,D.K., Ganesh,M., Ghosh,S., Bell,I., Gerhard,D.S., and Gingeras,T.R. (2005). Transcriptional maps of 10 human chromosomes at 5-nucleotide resolution. Science. *308*, 1149-1154.

Choo,A.Y., Yoon,S.O., Kim,S.G., Roux,P.P., and Blenis,J. (2008). Rapamycin differentially inhibits S6Ks and 4E-BP1 to mediate cell-type-specific repression of mRNA translation. PNAS *105*, 17414-17419.

Coller,H.A., Sang,L., and Roberts,J.M. (2006). A new description of cellular quiescence. PLoS. Biol. *4*, e83.

Cui,P., Lin,Q., Ding,F., Xin,C., Gong,W., Zhang,L., Geng,J., Zhang,B., Yu,X., Yang,J., Hu,S., and Yu,J. (2010). A comparison between ribo-minus RNA-sequencing and polyA-selected RNA-sequencing. Genomics. *96*, 259-265.

Dehlin,E., Wormington,M., Korner,C.G., and Wahle,E. (2000). Cap-dependent deadenylation of mRNA. EMBO J *19*, 1079-1086.

Doench,J.G., Petersen,C.P., and Sharp,P.A. (2003). siRNAs can function as miRNAs. Genes Dev. *17*, 438-442.

Doench,J.G. and Sharp,P.A. (2004). Specificity of microRNA target selection in translational repression. Genes Dev. *18*, 504-511.

Dreyfuss,G., Choi,Y.D., and Adam,S.A. (1984). Characterization of heterogeneous nuclear RNA-protein complexes in vivo with monoclonal antibodies. Mol. Cell Biol. *4*, 1104-1114.

Elias,J.E. and Gygi,S.P. (2007). Target-decoy search strategy for increased confidence in large-scale protein identifications by mass spectrometry. Nat Methods. *4*, 207-214.

Eng,J.K., McCormack,A.L., and Yates,J.R. (1994). An approach to correlate tandem mass spectral data of peptides with amino acid sequences in a protein database. J Am. Soc. Mass Spectrom. *5*, 976-989.

Fabian,M.R., Sundermeier,T.R., and Sonenberg,N. (2010). Understanding How miRNAs Post-Transcriptionally Regulate Gene Expression. Prog. Mol. Subcell. Biol. *50*, 1-20.

Feldman,M.E., Apsel,B., Uotila,A., Loewith,R., Knight,Z.A., Ruggero,D., and Shokat,K.M. (2009). Active-site inhibitors of mTOR target rapamycin-resistant outputs of mTORC1 and mTORC2. PLoS. Biol. *7*, e38.

Fonseca,B.D., Smith,E.M., Yelle,N., Alain,T., Bushell,M., and Pause,A. (2014). The ever-evolving role of mTOR in translation. Semin. Cell Dev Biol. *36*,102-12. doi: 10.1016/j.semcdb.2014.09.014.

Friedman,R.C., Farh,K.K., Burge,C.B., and Bartel,D.P. (2009). Most mammalian mRNAs are conserved targets of microRNAs. Genome Res. *19*, 92-105.

Friedman,Y. and Linial,M. (2013). miRror2.0: a platform for assessing the joint action of microRNAs in cell regulation. J Bioinform. Comput. Biol. *11*, 1343012.

Gingras,A.C., Gygi,S.P., Raught,B., Polakiewicz,R.D., Abraham,R.T., Hoekstra,M.F., Aebersold,R., and Sonenberg,N. (1999). Regulation of 4E-BP1 phosphorylation: a novel two-step mechanism. Genes Dev *13*, 1422-1437.

Hsieh,A.C., Liu,Y., Edlind,M.P., Ingolia,N.T., Janes,M.R., Sher,A., Shi,E.Y., Stumpf,C.R., Christensen,C., Bonham,M.J., Wang,S., Ren,P., Martin,M., Jessen,K., Feldman,M.E., Weissman,J.S., Shokat,K.M., Rommel,C., and Ruggero,D. (2012). The translational landscape of mTOR signalling steers cancer initiation and metastasis. Nature *485*, 55-61.

Hsu,P.P., Kang,S.A., Rameseder,J., Zhang,Y., Ottina,K.A., Lim,D., Peterson,T.R., Choi,Y., Gray,N.S., Yaffe,M.B., Marto,J.A., and Sabatini,D.M. (2011). The mTOR-regulated phosphoproteome reveals a mechanism of mTORC1-mediated inhibition of growth factor signaling. Science *332*, 1317-1322.

Huang,D.W., Sherman,B.T., and Lempicki,R.A. (2008). Systematic and integrative analysis of large gene lists using DAVID bioinformatics resources. Nat. Protocols *4*, 44-57.

Huttlin,E.L., Jedrychowski,M.P., Elias,J.E., Goswami,T., Rad,R., Beausoleil,S.A., Villen,J., Haas,W., Sowa,M.E., and Gygi,S.P. (2010). A tissue-specific atlas of mouse protein phosphorylation and expression. Cell. *143*, 1174-1189.

Jopling,C.L., Yi,M., Lancaster,A.M., Lemon,S.M., and Sarnow,P. (2005). Modulation of hepatitis C virus RNA abundance by a liver-specific MicroRNA. Science *309*, 1577-1581.

Karim,M.M., Svitkin,Y.V., Kahvejian,A., De,C.G., Costa-Mattioli,M., and Sonenberg,N. (2006). A mechanism of translational repression by competition of Paip2 with eIF4G for poly(A) binding protein (PABP) binding. Proc. Natl. Acad. Sci. U. S. A *103*, 9494-9499.

Kedde,M., Strasser,M.J., Boldajipour,B., Oude Vrielink,J.A., Slanchev,K., le,S.C., Nagel,R., Voorhoeve,P.M., van,D.J., Orom,U.A., Lund,A.H., Perrakis,A., Raz,E., and Agami,R. (2007). RNA-binding protein Dnd1 inhibits microRNA access to target mRNA. Cell *131*, 1273-1286.

Korner,C.G., Wormington,M., Muckenthaler,M., Schneider,S., Dehlin,E., and Wahle,E. (1998). The deadenylating nuclease (DAN) is involved in poly(A) tail removal during the meiotic maturation of Xenopus oocytes. EMBO J *17*, 5427-5437.

Kusov,Y.Y., Shatirishvili,G., Dzagurov,G., and Gauss-Muller,V. (2001). A new G-tailing method for the determination of the poly(A) tail length applied to hepatitis A virus RNA. Nucleic Acids Res. *29*, E57.

Lee,S., Truesdell,S.S., Bukhari,S.I., Lee,J.H., Letonqueze,O., and Vasudevan,S. (2014). Upregulation of eIF5B controls cell-cycle arrest and specific developmental stages. Proc. Natl. Acad. Sci. U. S. A *111*, E4315-E4322.

Lee,S.H. and McCormick,F. (2006). p97/DAP5 is a ribosome-associated factor that facilitates protein synthesis and cell proliferation by modulating the synthesis of cell cycle proteins. EMBO J. *25*, 4008-4019.

Levy-Strumpf,N., Deiss,L.P., Berissi,H., and Kimchi,A. (1997). DAP-5, a novel homolog of eukaryotic translation initiation factor 4G isolated as a putative modulator of gamma interferon-induced programmed cell death. Mol. Cell Biol. *17*, 1615-1625.

Ling,J., Morley,S.J., Pain,V.M., Marzluff,W.F., and Gallie,D.R. (2002). The histone 3'-terminal stem-loop-binding protein enhances translation through a functional and physical interaction with eukaryotic initiation factor 4G (eIF4G) and eIF3. Mol. Cell Biol. *22*, 7853-7867.

Liu,Q., Fu,H., Sun,F., Zhang,H., Tie,Y., Zhu,J., Xing,R., Sun,Z., and Zheng,X. (2008). miR-16 family induces cell cycle arrest by regulating multiple cell cycle genes. Nucleic Acids Res. *36*, 5391-5404.

Loayza-Puch,F., Drost,J., Rooijers,K., Lopes,R., Elkon,R., and Agami,R. (2013). p53 induces transcriptional and translational programs to suppress cell proliferation and growth. Genome Biol *14*, R32.

Marzluff,W.F., Wagner,E.J., and Duronio,R.J. (2008). Metabolism and regulation of canonical histone mRNAs: life without a poly(A) tail. Nat Rev. Genet. *9*, 843-854.

McAlister,G.C., Huttlin,E.L., Haas,W., Ting,L., Jedrychowski,M.P., Rogers,J.C., Kuhn,K., Pike,I., Grothe,R.A., Blethrow,J.D., and Gygi,S.P. (2012). Increasing the multiplexing capacity of TMTs using reporter ion isotopologues with isobaric masses. Anal. Chem. *84*, 7469-7478.

McAlister,G.C., Nusinow,D.P., Jedrychowski,M.P., Wuhr,M., Huttlin,E.L., Erickson,B.K., Rad,R., Haas,W., and Gygi,S.P. (2014). MultiNotch MS3 enables accurate, sensitive, and multiplexed detection of differential expression across cancer cell line proteomes. Anal. Chem. *86*, 7150-7158.

Meijer,H.A., Bushell,M., Hill,K., Gant,T.W., Willis,A.E., Jones,P., and de Moor,C.H. (2007). A novel method for poly(A) fractionation reveals a large population of mRNAs with a short poly(A) tail in mammalian cells. Nucleic Acids Res. *35*, e132.

Mili,S. and Steitz,J.A. (2004). Evidence for reassociation of RNA-binding proteins after cell lysis: implications for the interpretation of immunoprecipitation analyses. RNA. *10*, 1692-1694.

Moon,K.H., Zhao,X., and Yu,Y.T. (2006). Pre-mRNA splicing in the nuclei of Xenopus oocytes. Methods Mol. Biol. *322*, 149-163.

Moretti,F., Kaiser,C., Zdanowicz-Specht,A., and Hentze,M.W. (2012). PABP and the poly(A) tail augment microRNA repression by facilitated miRISC binding. Nat Struct. Mol. Biol *19*, 603-608.

Mortensen,R.D., Serra,M., Steitz,J.A., and Vasudevan,S. (2011). Posttranscriptional activation of gene expression in Xenopus laevis oocytes by microRNA-protein complexes (microRNPs). Proc. Natl. Acad. Sci. U. S. A *108*, 8281-8286.

Muranen,T., Selfors,L.M., Worster,D.T., Iwanicki,M.P., Song,L., Morales,F.C., Gao,S., Mills,G.B., and Brugge,J.S. (2012). Inhibition of PI3K/mTOR leads to adaptive resistance in matrix-attached cancer cells. Cancer Cell. *21*, 227-239.

Nelson,P.T., De Planell-Saguer,M., Lamprinaki,S., Kiriakidou,M., Zhang,P., O'Doherty,U., and Mourelatos,Z. (2007). A novel monoclonal antibody against human Argonaute proteins reveals unexpected characteristics of miRNAs in human blood cells. RNA. *13*, 1787-1792.

Nevins,T.A., Harder,Z.M., Korneluk,R.G., and Holcik,M. (2003). Distinct regulation of internal ribosome entry site-mediated translation following cellular stress is mediated by apoptotic fragments of eIF4G translation initiation factor family members eIF4GI and p97/DAP5/NAT1. J. Biol. Chem. *278*, 3572-3579.

Nousch,M., Reed,V., Bryson-Richardson,R.J., Currie,P.D., and Preiss,T. (2007). The eIF4G-homolog p97 can activate translation independent of caspase cleavage. RNA. *13*, 374-384.

Obad,S., dos Santos,C.O., Petri,A., Heidenblad,M., Broom,O., Ruse,C., Fu,C., Lindow,M., Stenvang,J., Straarup,E.M., Hansen,H.F., Koch,T., Pappin,D., Hannon,G.J., and Kauppinen,S. (2011). Silencing of microRNA families by seed-targeting tiny LNAs. Nat Genet *43*, 371-378.

Peculis,B.A. and Steitz,J.A. (1993). Disruption of U8 nucleolar snRNA inhibits 5.8S and 28S rRNA processing in the Xenopus oocyte. Cell *73*, 1233-1245.

Penalva,L.O., Burdick,M.D., Lin,S.M., Sutterluety,H., and Keene,J.D. (2004). RNA-binding proteins to assess gene expression states of co-cultivated cells in response to tumor cells. Mol. Cancer. *3*, 24.

Prives,C. and Foukai,D. (1991). Use of oligonucleotides for antisense experiments in Xenopus laevis oocytes. Methods Cell Biol. *36*, 185-210.

Radford,H.E., Meijer,H.A., and de Moor,C.H. (2008). Translational control by cytoplasmic polyadenylation in Xenopus oocytes. Biochim. Biophys. Acta *1779*, 217-229.

Ramirez-Valle,F., Braunstein,S., Zavadil,J., Formenti,S.C., and Schneider,R.J. (2008). eIF4GI links nutrient sensing by mTOR to cell proliferation and inhibition of autophagy. J Cell Biol *181*, 293-307.

Rassa,J.C., Wilson,G.M., Brewer,G.A., and Parks,G.D. (2000). Spacing constraints on reinitiation of paramyxovirus transcription: the gene end U tract acts as a spacer to separate gene end from gene start sites. Virology *274*, 438-449.

Riley,K.J., Yario,T.A., and Steitz,J.A. (2012). Association of Argonaute proteins and microRNAs can occur after cell lysis. RNA. *18*, 1581-1585.

Rissland,O.S., Hong,S.J., and Bartel,D.P. (2011). MicroRNA destabilization enables dynamic regulation of the miR-16 family in response to cell-cycle changes. Mol. Cell *43*, 993-1004.

Roberts,A.P., Lewis,A.P., and Jopling,C.L. (2011). miR-122 activates hepatitis C virus translation by a specialized mechanism requiring particular RNA components. Nucleic Acids Res. *39*, 7716-29.

Salles,F.J., Richards,W.G., and Strickland,S. (1999). Assaying the polyadenylation state of mRNAs. Methods *17*, 38-45.

Sang,L., Coller,H.A., and Roberts,J.M. (2008). Control of the reversibility of cellular quiescence by the transcriptional repressor HES1. Science *321*, 1095-1100.

Seal,R., Temperley,R., Wilusz,J., Lightowlers,R.N., and Chrzanowska-Lightowlers,Z.M. (2005). Serum-deprivation stimulates cap-binding by PARN at the expense of eIF4E, consistent with the observed decrease in mRNA stability. Nucleic Acids Res. *33*, 376-387.

Selbach,M., Schwanhausser,B., Thierfelder,N., Fang,Z., Khanin,R., and Rajewsky,N. (2008). Widespread changes in protein synthesis induced by microRNAs. Nature *455*, 58-63.

Siomi,M.C., Zhang,Y., Siomi,H., and Dreyfuss,G. (1996). Specific sequences in the fragile X syndrome protein FMR1 and the FXR proteins mediate their binding to 60S ribosomal subunits and the interactions among them. Mol. Cell Biol. *16*, 3825-3832.

Smith,R.W. and Gray,N.K. (2010). Poly(A)-binding protein (PABP): a common viral target. Biochem. J. *426*, 1-12.

Sonenberg,N. and Hinnebusch,A.G. (2009). Regulation of translation initiation in eukaryotes: mechanisms and biological targets. Cell *136*, 731-745.

Subtelny,A.O., Eichhorn,S.W., Chen,G.R., Sive,H., and Bartel,D.P. (2014). Poly(A)-tail profiling reveals an embryonic switch in translational control. Nature. *508*, 66-71.

Sun,X., Gao,L., Chien,H.Y., Li,W.C., and Zhao,J. (2013). The regulation and function of the NUAK family. J Mol. Endocrinol. *51*, R15-R22.

Thoreen,C.C., Chantranupong,L., Keys,H.R., Wang,T., Gray,N.S., and Sabatini,D.M. (2012). A unifying model for mTORC1-mediated regulation of mRNA translation. Nature *485*, 109-113.

Thoreen,C.C., Kang,S.A., Chang,J.W., Liu,Q., Zhang,J., Gao,Y., Reichling,L.J., Sim,T., Sabatini,D.M., and Gray,N.S. (2009). An ATP-competitive mammalian target of rapamycin inhibitor reveals rapamycin-resistant functions of mTORC1. J. Biol. Chem. *284*, 8023-8032.

Ting,L., Rad,R., Gygi,S.P., and Haas,W. (2011). MS3 eliminates ratio distortion in isobaric labeling-based multiplexed quantitative proteomics. Nat Methods *8*, 937-940.

Tolonen,A.C. and Haas,W. (2014). Quantitative proteomics using reductive dimethylation for stable isotope labeling. J Vis. Exp. *89*, doi: 10.3791/51416.

Truesdell,S.S., Mortensen,R.D., Seo,M., Schroeder,J.C., Lee,J.H., Letonqueze,O., and Vasudevan,S. (2012). MicroRNA-mediated mRNA Translation Activation in Quiescent Cells and Oocytes Involves Recruitment of a Nuclear microRNP. Sci. Rep. *2*, 842.

Vasudevan,S. and Steitz,J.A. (2007). AU-rich-element-mediated upregulation of translation by FXR1 and Argonaute 2. Cell *128*, 1105-1118.

Vasudevan,S., Tong,Y., and Steitz,J.A. (2007). Switching from repression to activation: microRNAs can up-regulate translation. Science *318*, 1931-1934.

Vasudevan,S., Tong,Y., and Steitz,J.A. (2008). Cell-cycle control of microRNA-mediated translation regulation. Cell Cycle *7*, 1545-1549.

Wang,F., Fu,X.D., Zhou,Y., and Zhang,Y. (2009). Down-regulation of the cyclin E1 oncogene expression by microRNA-16-1 induces cell cycle arrest in human cancer cells. BMB. Rep. *42*, 725-730.

Wang,Y. and Wang,Z. (2015). Efficient backsplicing produces translatable circular mRNAs. RNA. *21*, 172-179.

Weinmann,L., Hock,J., Ivacevic,T., Ohrt,T., Mutze,J., Schwille,P., Kremmer,E., Benes,V., Urlaub,H., and Meister,G. (2009). Importin 8 is a gene silencing factor that targets argonaute proteins to distinct mRNAs. Cell *136*, 496-507.

Wilusz,J.E., JnBaptiste,C.K., Lu,L.Y., Kuhn,C.D., Joshua-Tor,L., and Sharp,P.A. (2012). A triple helix stabilizes the 3' ends of long noncoding RNAs that lack poly(A) tails. Genes Dev. *26*, 2392-2407.

Wu,L., Fan,J., and Belasco,J.G. (2006). MicroRNAs direct rapid deadenylation of mRNA. Proc. Natl. Acad. Sci. U. S. A *103*, 4034-4039.

Yanagiya,A., Delbes,G., Svitkin,Y.V., Robaire,B., and Sonenberg,N. (2010). The poly(A)-binding protein partner Paip2a controls translation during late spermiogenesis in mice. J. Clin. Invest *120*, 3389-3400.

Yang,L., Duff,M.O., Graveley,B.R., Carmichael,G.G., and Chen,L.L. (2011). Genomewide characterization of non-polyadenylated RNAs. Genome Biol. *12*, R16-12.

Yang,Z., Jakymiw,A., Wood,M.R., Eystathioy,T., Rubin,R.L., Fritzler,M.J., and Chan,E.K. (2004). GW182 is critical for the stability of GW bodies expressed during the cell cycle and cell proliferation. J. Cell Sci. *117*, 5567-5578.

Yehudai-Resheff,S. and Schuster,G. (2000). Characterization of the E.coli poly(A) polymerase: nucleotide specificity, RNA-binding affinities and RNA structure dependence. Nucleic Acids Res. *28*, 1139-1144.

Yu,J.H., Yang,W.H., Gulick,T., Bloch,K.D., and Bloch,D.B. (2005). Ge-1 is a central component of the mammalian cytoplasmic mRNA processing body. RNA. *11*, 1795-1802.

Zhang,X., Devany,E., Murphy,M.R., Glazman,G., Persaud,M., and Kleiman,F.E. (2015). PARN deadenylase is involved in miRNA-dependent degradation of TP53 mRNA in mammalian cells. Nucleic Acids Res. *43*, 10925-38.